spoor

Pilot Report

Spoor AI - Offshore Avian Monitoring by Buoy

Experiences and Future Potential

June - October 2023

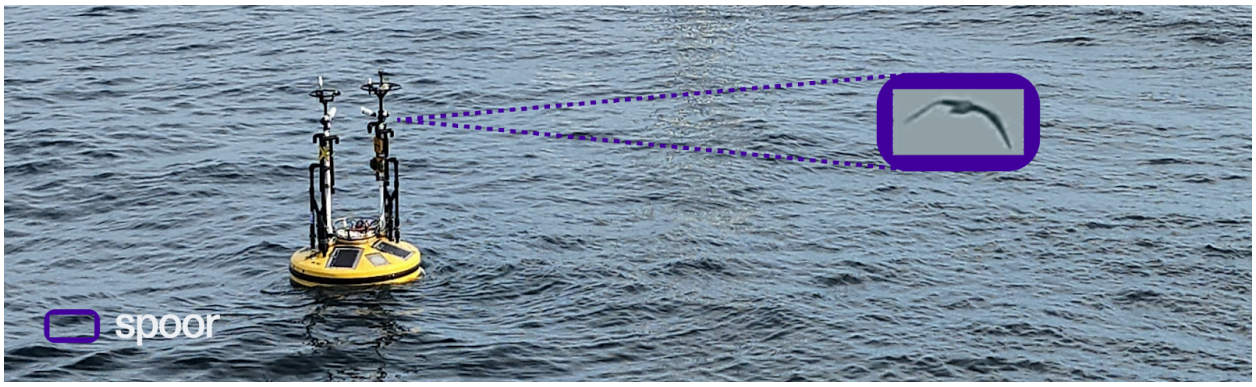

Summary

Location: Hywind Tampen Floating Windfarm Norway

Number of cameras: Four

Days of data analysed: 127

Hours of video analysed: 4,880

Hours of unique bird detections: 52.1

Total bird detections: 55,868

Red list *endangered* birds identified: Black-legged Kittiwake

Red list *vulnerable* birds identified: European Herring Gull

Table of contents

Introduction

The primary purpose of this report is to document the technical performance of Spoor's pioneering offshore pre-construction bird monitoring solution. By mounting cameras on a multi-sensor Fugro buoy and deploying Spoor's AI software to detect and track birds, a range of new possibilities emerge to capture bird activity data far offshore – but this type of platform and environment also create new challenges. Cameras are subjected to challenging environmental conditions far outside the scope of previous installations (on a turbine service platform for example), and are practically inaccessible by humans for long periods of time, requiring extremely robust hardware, and limiting access to data during deployment. The buoy also moves dynamically with the wind and waves, which requires an evolution of methods to interpret the data. This pilot demonstrates how these challenges manifested and have been managed.

Although the analysis of the biodiversity data itself is not the primary purpose of this report, these data are also very interesting and have the potential to provide entirely new insights about bird activity in the area and to highlight the potential nature-positive impact of this technology when applied at scale.

Hywind Tampen

Hywind Tampen is the largest floating wind farm in the world, located 140 km off the Norwegian coast (see Figure 1) with a capacity of 88MW, provided by eleven 8.6MW Siemens Gamesa wind turbines. The project directly reduces emissions from oil and gas production on the Snorre and Gullfaks offshore fields by 200,000 tonnes of CO_2 and 1,000 tonnes of NOx emissions per year. Hywind Tampen is also Norway's first full scale offshore wind farm and has a critically important role to play in the development of the Norwegian offshore wind industry and the global expansion of floating offshore wind. From a biodiversity perspective, Hywind Tampen provides a unique opportunity to gather bird activity data off the coast of Norway and start building a knowledge base to understand and protect species as they interact with industrial windfarm development.

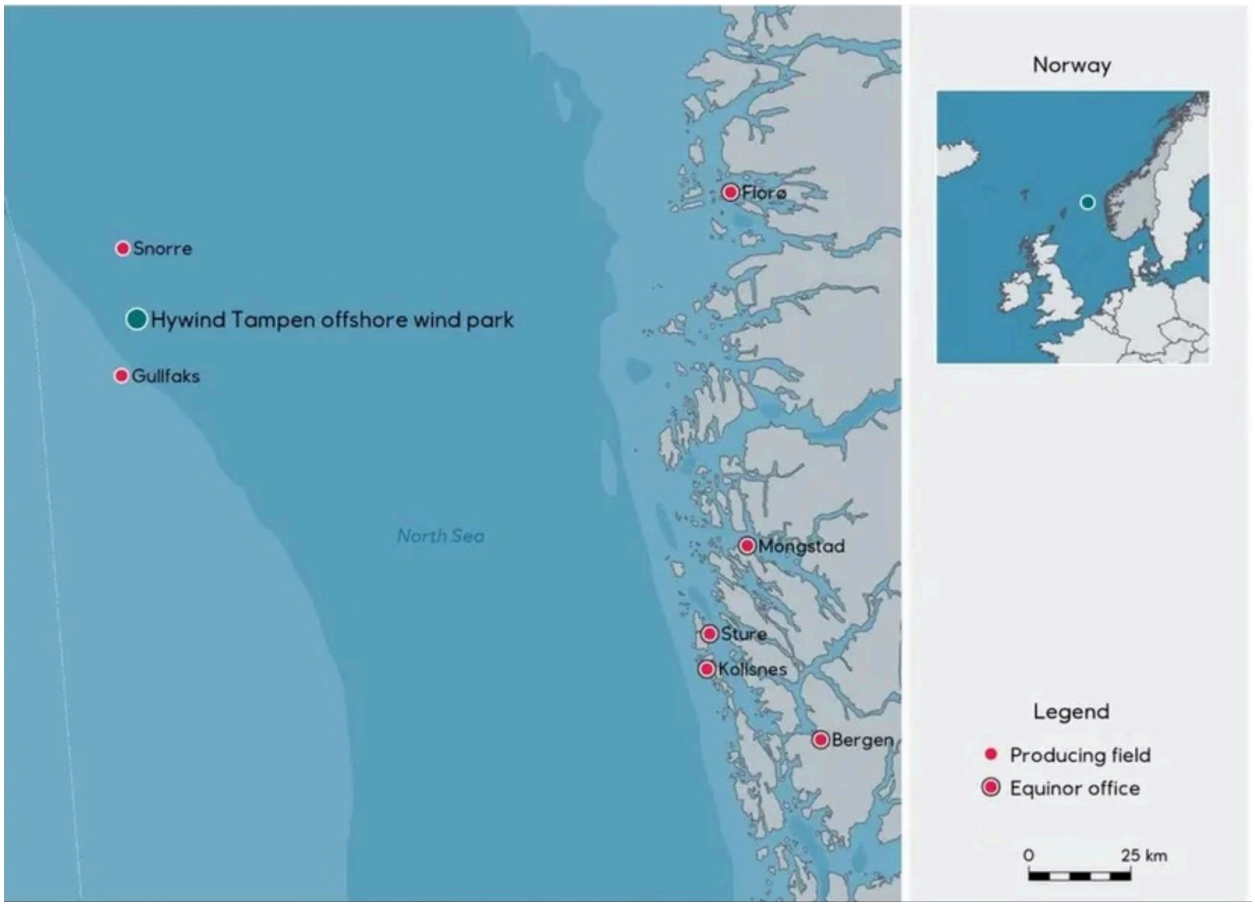

Figure 1: Illustration retrieved from Equinor: Hywind Tampen (n.d)*, showing the location of the Hywind Tampen wind farm, 140 km off the Norwegian west coast.*

About Spoor

Spoor is a Norwegian biodiversity technology company founded in 2020, with a vision to enable nature and industry to coexist. Spoor promotes biodiversity positive wind energy development by combining high-resolution video cameras as sensors with advanced AI-based software to detect, identify and analyse bird activity. Such accurate and trusted biodiversity insight will reduce environmental risks and allow smarter decision making both for industry and regulators. Spoor currently employs 22 people of diverse backgrounds; with 14 nationalities and a 36% female representation, their expertise includes ornithology, wind power, regulatory affairs, data science, edge computing, and machine learning. Since the first pilot was launched in March 2021, Spoor's solution has been deployed on multiple onshore and offshore sites in Northern Europe, with further installations underway. A list of Spoor's projects can be seen in the Appendix. Together with Equinor and Fugro, Spoor has pioneered the use of floating offshore platforms offshore to monitor bird-activity for pre-construction surveys.

Bird detection and tracking

The Spoor AI

Spoor's Artificial Intelligence (AI) software analyses all recorded hours of video in order to detect and track birds. Any bird appearing for more than 1 second in the camera field of view is detected and tracked. The output is a video combined with a visual image of the flight trajectory, complemented by still images of the bird at certain times during the flight. In addition, statistics on temporal distribution, flight height, species, and abundance correlated to wind speed and -direction are presented to users in the Spoor AI webapp (app.spoor.ai).

At the time of writing, Spoor AI software has been trained to identify individual birds. If several birds appear simultaneously in the field of view - either because they fly in a flock, or because they happened to be active at the same time - the AI will detect and display their separate flight paths.

A novel AI model has been developed for this pilot, based on the principle of detecting objects instead of detecting movement. The AI can handle the rapidly changing horizon line, and can detect birds that appear in front of the sea.

AI performance: accuracy, precision and recall

Within machine learning and artificial intelligence, quality is measured by accuracy, as explained in *Evidently AI: Accuracy vs. precision vs. recall in machine learning: what's the difference?* (n.d). Simply put, it expresses how often the AI is correct. Correct detections are birds that the AI marked as "bird", and non-birds (e.g. an airplane) that the AI marked as "non-bird". These are called true positives and true negatives, respectively. Incorrect detections are birds that the AI marked as "non-bird", and non-birds that the AI marked as "bird". These are called false negatives and false positives, respectively. Accuracy is calculated by dividing the sum of correct (true) detections on the sum of all detections (false and true).

Precision is an expression of how often the AI is correct when it claims to have detected a bird. It is calculated by the number of true positives divided by all positives. Recall is the percentage of the birds the AI manages to detect. Recall is calculated by dividing the number of true positives by the sum of true positives and false negatives, and is discussed in more detail in the *Comparing to a Ground Truth* chapter.

In theory, all the three metrics can reach 100%, but in practice, this is very rarely the case. In most real-life situations, there is for example a tradeoff between optimising precision and optimising recall. Optimising for precision means requiring the AI to be correct almost every time it marks an observation as "bird". In order to achieve a high precision, the AI may disregard observations it is less certain about, with the potential result that a larger number of real birds were marked as "non-bird". The recall is the measure of how many real birds the AI detects, so a higher number of real birds marked as "non-bird" will negatively affect the recall metric.

The definition of a good accuracy level within machine learning depends on the context. Both precision and recall are useful to understand different aspects of the AI. Still, Accuracy is commonly used as the primary quality metric.

Reasons for false detections

False (incorrect) detections are birds that the AI marked as "non-bird", and non-birds that the AI marked as "bird". These are called false negatives and false positives, respectively. The reason for false negatives (birds being missed) are discussed more in the *Comparing to a Ground Truth* chapter. False positives are sometimes called *noise*, and can be insects or other moving objects that resemble the movement of a distant bird, like airplanes or helicopters. Other phenomena that can be interpreted as a bird by the AI is sun reflections on impurities on the lens and certain cloud formations. The reason for these false detections is connected to the specific identifiers that the AI has been trained to recognize, and is constantly improved due to the self-learning nature of the AI.

Quality assurance

In order to ensure high levels of quality, Spoor deploys a number of techniques.

- Spoor prioritises building high-quality AI training data sets. Due to the increasing number of on-site deployments, Spoor has a large and varied asset of raw data. The raw data are processed and refined into unique, high-quality training data sets that feed into the AI. Data processing and refinement is done with advanced tools combined with the biological expertise of Spoor's in-house ornithologist.
- The AI assigns a confidence to detections. If the confidence drops below a certain threshold, the data is manually verified by trained members of staff. Due to the self-learning nature of the AI system, the confidence levels increase over time.
- Several times per week, a sample of about 2% of all new detections are sent for manual verification in order to monitor the general levels of false and true positives. The self-learning nature of the AI ensures that the level of false positives diminish over time.
- Spoor also conducts regular in-field verifications to measure false negatives. See more in the Comparing to a Ground Truth chapter below.

Comparing to a ground truth

Spoor conducts quality verifications by comparing Spoor AI results to the field observations of a human observer, usually a trained ornithologist. This is done at different sites to ensure quality is measured across various environments.

In this method, the human observer visits a site and manually records bird detections within a field of view that match the field of view of the camera used for Spoor data collection.

The bird detections are noted down with information on: time of the bird entering the field of view and exiting the field of view, the bird's trajectory through the field of view, and its species. If

the verification focus is spatial mapping, the human observer records flight height and distance from the observation point. In order for this to be precise, the ornithologist uses an instrument like a laser rangefinder or binoculars with rangefinders. This data set represents a "Ground Truth"; information that is known to be real or true, provided by direct observation and measurement (i.e. empirical evidence).

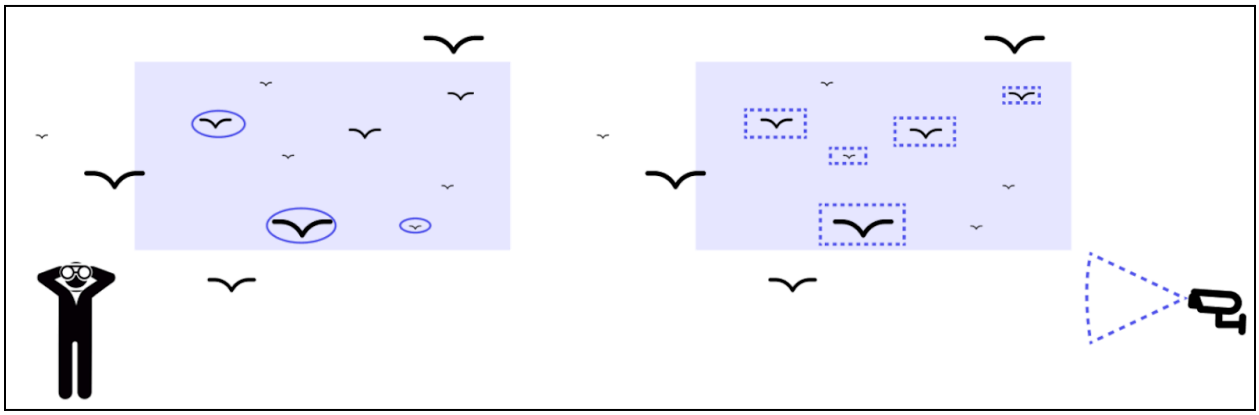

Figure 2: Combining the results of a human observer (left) and the Spoor AI (right) yields a Ground Truth dataset that can be used for assessing the performance of both the human observer and Spoor AI.

The Ground Truth data set is subsequently compared with the Spoor AI detections. Because the human observer is also subject to errors, some birds are missed by the human observer but are detected by the Spoor AI. The number of birds missed by humans are determined in the comparison, and added to the Ground Truth data set. This yields a "more true" ground truth than would be achieved by only taking the manual observations as the ground truth. In this way, it serves as a cross-verification of both the Spoor AI and the manual observer, allowing for assessing quality and levels of error of both methods.

Sampling method

Spoor's method is based on observations in a predetermined spatial frame of reference, called Eulerian sampling as explained in Phillips *et al*. (2019). One effect of the Eulerian reference frame is that one cannot track individuals as they leave the reference frame. Each time a bird enters the field of view, it is counted as one observation, and it is not possible to determine whether this individual has been observed before or not. A high number of bird observations does not automatically equal a high abundance of birds. In other words, it is measuring activity levels rather than actual abundance. This is an inherent feature of both a stationary and a moving observer regardless of technology; be it camera-based, manual observer or radar. It is simply an effect of the reference frame of monitoring being a particular spatial volume, and not the bird population as such. If bird populations, or individual members, are the subject for the research, bio-logging methods are more suited, for example bird ringing or GPS tracking. This is termed Lagrangian sampling. Both Eulerian and Lagrangian approaches are vulnerable to uncertainty and/or bias in measurement and sampling.

Range

An inherent effect of any observation method based on electromagnetic radiation, is that larger objects are detectable over longer distances than smaller objects. This applies to devices like visual spectrum and thermal cameras, radars, telescopes, and the human eye. Intuitively, we know that the leaf of a tree is a small object that is only visible over a few metres with the human eye, while the moon is a very large object that is visible over hundreds of thousands of kilometres.

For this reason, large birds are detectable over a longer distance than smaller birds. When discussing detection range, bird size needs to be taken into account.

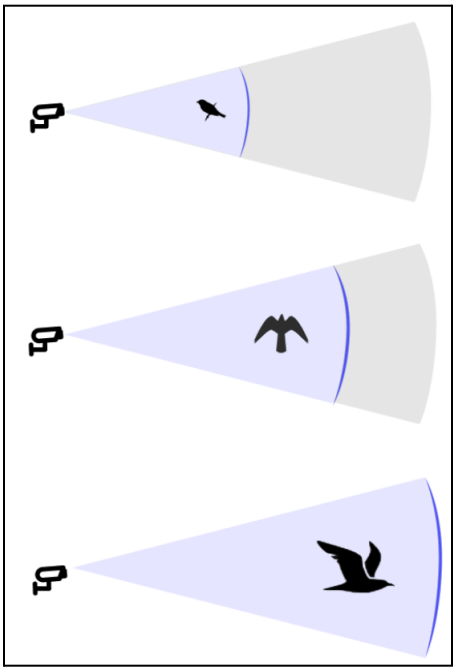

Figure 3: The detection range depends on a number of variables, including the size of the observed birds. In general, large birds are detectable over a longer distance than smaller birds.

The maximum detection range also depends on the properties of the sensor equipment. For a mid-range camera with a standard lens, a bird with a wing span of 150 cm (like a Great Black-Backed Gull) can in theory be detected up to 2 km away, while a bird with a 25 cm (like a Meadow Pipit) can be detected up to 350 m away. Increasing the lens zoom capabilities and/or the camera resolution will yield greater ranges.

Because the purpose of the monitoring in most cases is to get consistent knowledge on bird behaviour within a space that is planned for wind development or under operation, it is not only the range (distance), but the volume that is of importance. The surveyed space is a function of the range, height and width of the camera field of view. The effective volume - like range - depends on the bird size and camera properties and settings. The volume can be increased by increasing the range, but also by increasing the height and width of the field of view by selecting appropriate lens types and camera settings.

Flight heights

For single-camera sampling, the location of a bird can be derived from an image with both altitude and lateral and longitudinal position, based on the size of the bird and its relative location within the image. The bird size is preferably found by using an average measure for the size of the species it belongs to. For example, the body size of a Great Black-Backed Gull is 64-78 cm long, with a wingspan of 150-165 cm, according to *The Royal Society for the Protection of Birds: Great Black-backed Gull (n.d.)*.

In general, the uncertainty in the position is driven by a combination of factors such as pixelation (a property of the camera), variation in body size within each species, and variation in body orientation.

The bird size can be estimated by using an approximate average bird size. This is the current method used by Spoor, but it includes a larger uncertainty because the true bird size varies between species; from just a few centimetres to more than two metres in wingspan. The uncertainty in the bird size translates into a less accurate spatial position. As a next step, Spoor can calculate spatial positions per bird species, thus greatly reducing the measurement uncertainty.

Cameras mounted on a moving foundation pose an additional challenge in the calculation of the spatial positions of birds. As long as the horizon is in the field of view, it serves as a reference point for the calculation of a bird's flight height. However, for buoy-based cameras, the horizon is sometimes outside the field of view. Spoor has therefore developed a proprietary AI-based algorithm to estimate the camera orientation. The algorithm handles temporary disappearance of the horizon from the view and works in a variety of weather and lightning conditions. In this way, the flight height of all observed birds can be calculated.

Flight height can be used to inform the risk of bird collision with a turbine. Spoor provides a distribution of the flight height of the observed birds, where the height is given in metres above the sea level. The flight height of birds being tracked can be represented in numerous ways. In this pilot, Spoor calculates a flight height density by calculating the flight heights of all observed birds. Because the camera is in motion, the total vertical field of view is 75°, with 40° covered at any given point in time. A random sample of raw videos is used to derive the probability of all angles in the total field of view to be in the actual field of view. This probability distribution is then used to normalise the flight heights. This reduces the bias from both the motion of the camera and the pyramid shape of the camera's field of view. Finally, the normalised flight height density is grouped into 5 metre height bins.

Taxonomic classifications

The taxonomy levels considered in this report are order, family and species. The genus level has not been considered.

Classification is done by analysing the full-length track of the bird in question. The duration of a bird track can be from a few seconds and up to the full duration of a video file; usually five minutes. In order to determine the taxonomy of detected birds, some type of unique characteristic needs to be exhibited and visible. Characteristic can be the visual appearance of the bird (e.g. body- , wing- or tail shape, colours and patterns), flight characteristics (e.g. flight pattern, flight height, speed, flock behaviour, flapping frequency), and/or environmental factors (e.g. time of day, light or wind conditions). This imitates the way human observers classify birds.

There is no set level of frames needed in order to classify a bird, because the ease and speed of classification depends on the camera properties, visibility and bird characteristics. Some birds are easy to identify due to distinct characteristics which can be observed over large distances. Gulls, common swifts and European Starlings are examples of families and species that exhibit such "long-range" characteristics . Other birds have identifiers that require closer inspection. For example, certain species within the gull family exhibit very similar characteristics, and differentiating these requires higher resolution and/or closer proximity. This is also true for e.g. human observers.

The White-tailed Eagle is a species that exhibits unique characteristics in appearance, and Spoor AI has been trained to identify this species. New species will be trained according to demand. For this pilot, the classification is done by Spoor's in-house ornithologist. This quality-assured data is used to train the Spoor AI to recognize species automatically.

Sample selection for taxonomic classification

In order to determine taxonomy, more of the bird characteristics need to be visible compared to just detecting whether it is a bird or not. Thus, a portion of the AI bird detections will be so distant that its characteristic features are not distinguishable.

For this reason, a subset of the total detection sample has been selected for manual taxonomy classification. A criteria was set for the bird body to cover a minimum number of pixels. All bird detections above this threshold were part of the sample, ensuring representativeness and not introducing any new bias in the data set.

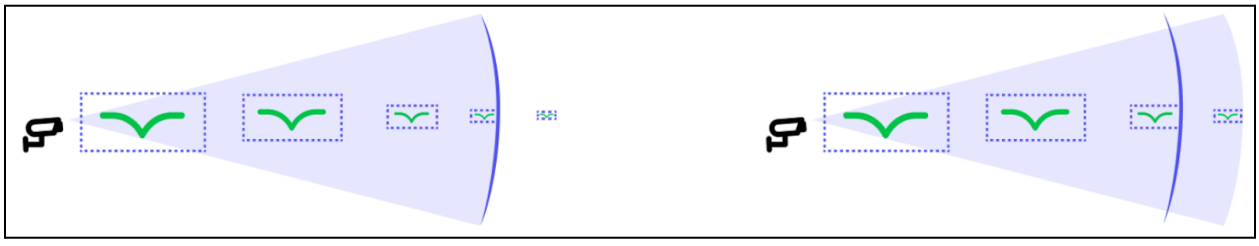

Figure 4: Illustration of the method for selecting detections that will undergo taxonomy determination. Any bird will appear large when it is close to the camera, and smaller when it is farther away from the camera. At a certain point, it will be outside the detection threshold (left) and will not be observed. When determining taxonomy, the bird needs to appear with a certain size so that characteristic features are visible (right) and the threshold is set so that birds appearing very small will not be included in the sample sent for taxonomy determination.

Method

Data capture

Surveillance cameras as sensors

Spoor AI utilises cameras as sensors for data capture. The Spoor AI software is hardware agnostic and can ingest video from any commercially available high-resolution camera. This allows for a flexible, lightweight and cost-effective infrastructure. The AI software is adapted to analyse data from both steady and non-steady vantage points, the latter being particularly relevant for offshore floating facilities.

Camera-based monitoring is a non-intrusive technology that will typically not interfere with any other installations. It is also a non-intrusive *methodology* that has minimal interference with the environment and species it is monitoring, and therefore introduces a minimum of sampling biases compared to e.g. human observers.

So far, Spoor has worked with surveillance video cameras from multiple suppliers, using both wide-angle dome cameras and classic “bullet” surveillance cameras as seen in Figure 5. Surveillance cameras are affordable and are designed to record continuously for periods of months to years. They have custom built water- and weatherproof housings that are durable in tough weather conditions throughout the seasons. A disadvantage is that they are designed for security rather than scientific purposes, so that certain settings (like focus and focal length, frame rate per second, multi-camera time syncs) are simplified and need to be adjusted by Spoor’s engineers. However, both these settings and the general quality and performance of the cameras are being improved by the camera manufacturers on a continuous basis.

The choice of camera, lens, housing and other equipment is decided on a case-by-case basis. Various aspects like cost, durability in different environments, focal distance, and field of view need to be considered in relation to the project specific purpose of monitoring.

A number of variables within the equipment determine the ability and quality of bird detection, some examples being sensor resolution, focal length, lens “speed” (f-stop), shutter speed, frame rate (Frames Per Second, FPS), and data bitrates.

Using cameras for data capture yields both advantages and limitations. Some of the limitations are:

- Visible Imaging Sensor cameras require daylight. For 24 hour monitoring they can be combined with thermal imaging cameras.
- Image quality is affected by weather; fog, rain and snow will typically reduce the range. Direct sun striking an unclean lens can also degrade the image quality. In addition,

atmospheric quality like humidity, airborne dust or air pollution affects image quality especially the onshore

- Range is ultimately restricted by the physics of lenses and the stability of the mounting location. The longer the focal length, the more likely any vibration will degrade the final video image (e.g. from wind against the camera body, or the vibration of a working wind turbine).

Camera models and settings

A total of four cameras were used in order to achieve a 360 degree field of view when mounted on the Fugro buoy, as seen in Figure 6. This pilot deployment was an opportunity to test different camera types, and two “bullet” cameras and two “dome” cameras were selected for a side by side comparison.

The “bullet” type camera is a “classic” surveillance camera, as seen in Figure 5. The model was AXIS Q1798-LE, which is a conventional and affordable high resolution camera. The dome type camera has a circular shape as seen in Figure 5, and is designed for more durability (it is specifically marine-grade). The selected model was AXIS Q3538-SLVE. Dome cameras also have a wider field of view compared to bullet cameras.

Figure 5: The bullet camera (left) of model AXIS Q1798-LE, and the dome camera (right) of model AXIS Q3538-SLVE. Images retrieved from AXIS Q1798-LE Network Camera (n.d) *and* AXIS Q3538-SLVE Dome Camera (n.d).

For this pilot report, the two dome cameras will be identified as Camera 1 and Camera 2 and the two bullet cameras will be identified as Camera 3 and Camera 4.

	Dome cameras	Bullet cameras
Camera number used in this report	Camera 1 Camera 2	Camera 3 Camera 4
Model	AXIS Q3538-SLVE	AXIS Q1798-LE
Focal length	7.875 mm (25% zoom)	12mm (0% zoom)
Frame rate	25 FPS	25 FPS
Estimated detection distance for bird of 1m wingspan	210 m	200 m
Estimated max detection height for bird of 1m wingspan	170 m	170 m
Horizontal scene width	85°	90°
Estimated max scene width	290 m	280 m
Estimated max detection space for bird of 1m wingspan	10.3×10^6 m^3	9.5×10^6 m^3

Table 2: The camera models, settings, and estimated bird detection ranges.

Camera installation on the buoy

Fugro's engineers connected the camera system to the buoy. The cameras were mounted on two poles as shown in Figure 6. The cameras were mounted around 3 metres above the water line.

Figure 6: The Fugro SEAWATCH buoy in the workshop prior to deployment. The bird monitoring cameras are installed at the two poles. Pictures taken March 2023 by Felix Kelberlau, Fugro.

The mounting position and the field of view of each camera is illustrated in Figure 7. Each of the cameras had a horizontal field of view of approximately 90°. The two dome cameras were mounted towards one side, and the two bullet cameras were pointing towards the other side. Examples of the fields of view for each camera are seen in Figures 10-13. As the buoy moves freely, the orientation of the fields of view will change almost constantly.

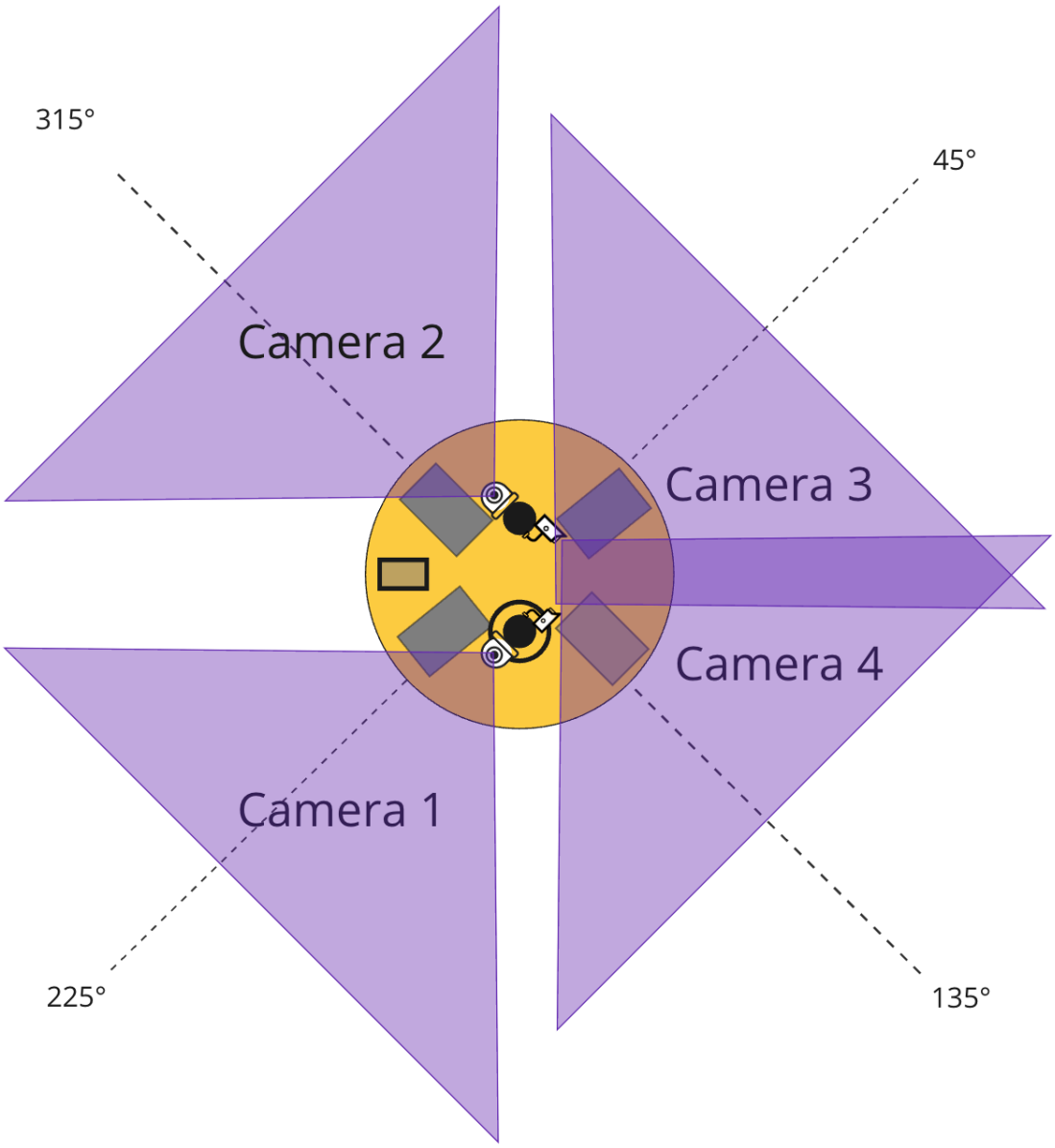

Figure 7: A sketch of the buoy (yellow circle) seen from the top, with the orientation of the field of view of each camera indicated by purple areas, relative to the buoy yaw. The actual camera ranges are not accurately represented in this sketch. Each of the angles of the horizontal field of view were approximately 90° per camera, as per Table 2.

Weather data

Weather data was retrieved from *The Norwegian Centre for Climate Services: Observations and weather statistics* (n.d.), from the meteorological station located at Gullfaks C, approximately 10 km south of the Hywind Tampen wind farm. The station is 80 metres above sea level.

This source provides a granular time series of wind direction, wind speed, air and sea

temperature, visibility, and cloud cover, but it does not give data on precipitation. Wind is defined in terms of the direction the wind is coming from.

Data storage and transfer

The buoy model was Fugro's SEAWATCH wind lidar buoy. The purpose of this buoy is typically to measure wind profiles, waves and current profiles, however Fugro is increasingly adding environmental and biodiversity sensors to these buoys to capture additional valuable data during these campaigns (acoustic recorders and cameras to detect bats, birds and marine mammals). The data capture and storage equipment used for bird monitoring were retrofitted by Fugro's engineers.

Physical space and power are limited resources on a buoy. They are typically deployed in remote offshore locations, and because maintenance visits are expensive, they should be able to work uninterrupted for several consecutive months, in rough environmental conditions. There is also very often a limited internet connection to transmit data, and for this reason the captured data has to be stored on the buoy (particularly true for video cameras which produce large volumes of high-resolution data). The data storage equipment had to be optimised for large data amounts, low power consumption and physical durability.

The selected data storage consisted of a Network Attached Storage (NAS) from Synology, DiskStation DS620slim. The NAS was fitted with six 8 TB Solid State hard Drives (SSD), providing a total of 48 TB storage. In addition to the NAS, each camera was equipped with a memory card of 1 TB each as backup storage.

Fugro's engineers connected the camera equipment to a control system, allowing for automated activation and deactivation of the equipment. The data capture was programmed to be active for specific times during daylight hours, ensuring that no periods of darkness were unnecessarily captured and stored.

The data pipeline is visualised in Figure 8. Data was stored on the buoy during the full measurement period. After buoy retrieval back to land, the hard drive was retrieved by Fugro's engineers and the data uploaded to Spoor's cloud storage. Spoor subsequently carried out data processing, AI bird detection, tracking and identification.

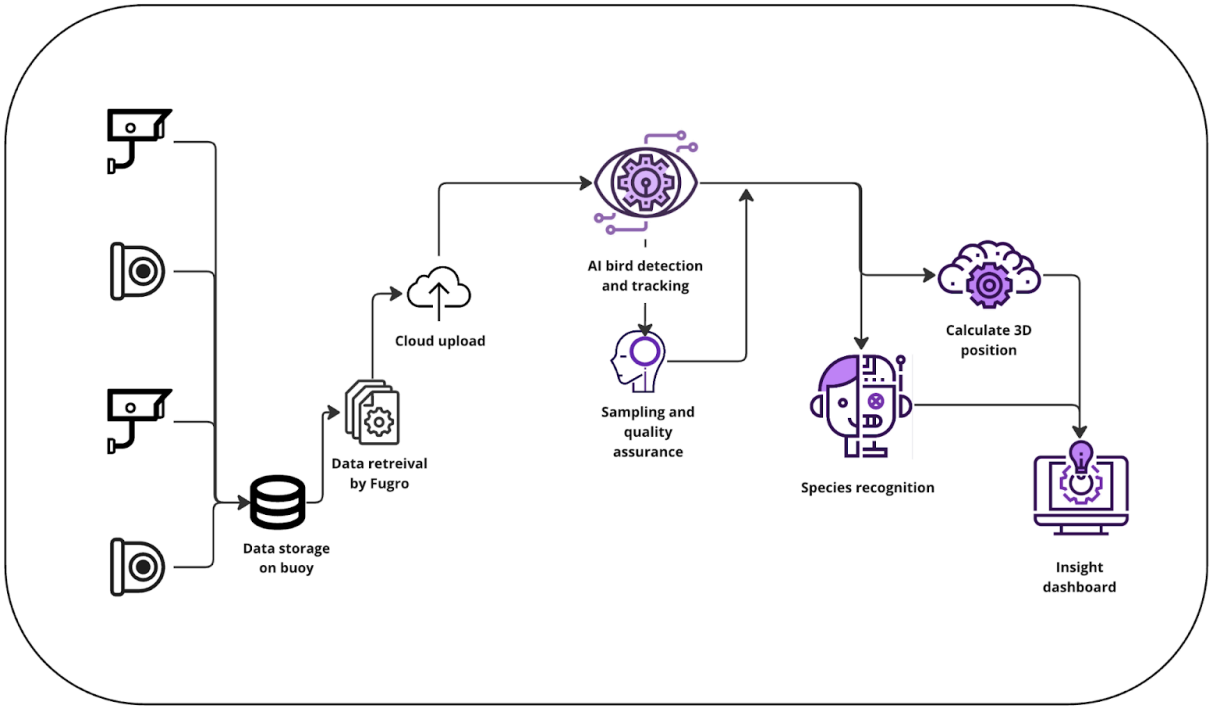

Figure 8: The data flow, storage and processing from data capture (left) to result visualisation (right). Data was captured and stored on the Fugro buoy, and Fugro staff retrieved the harddisk which were subsequently shipped to Spoor.

Vantage point

The buoy was located at 61°18'39.8"N 2°15'19.3"E. The location was at the south-western edge of the Hywind Tampen wind farm, between turbines HY07 and HY08, as illustrated in Figure 9. The buoy mooring has been designed to provide free movement of the buoy.

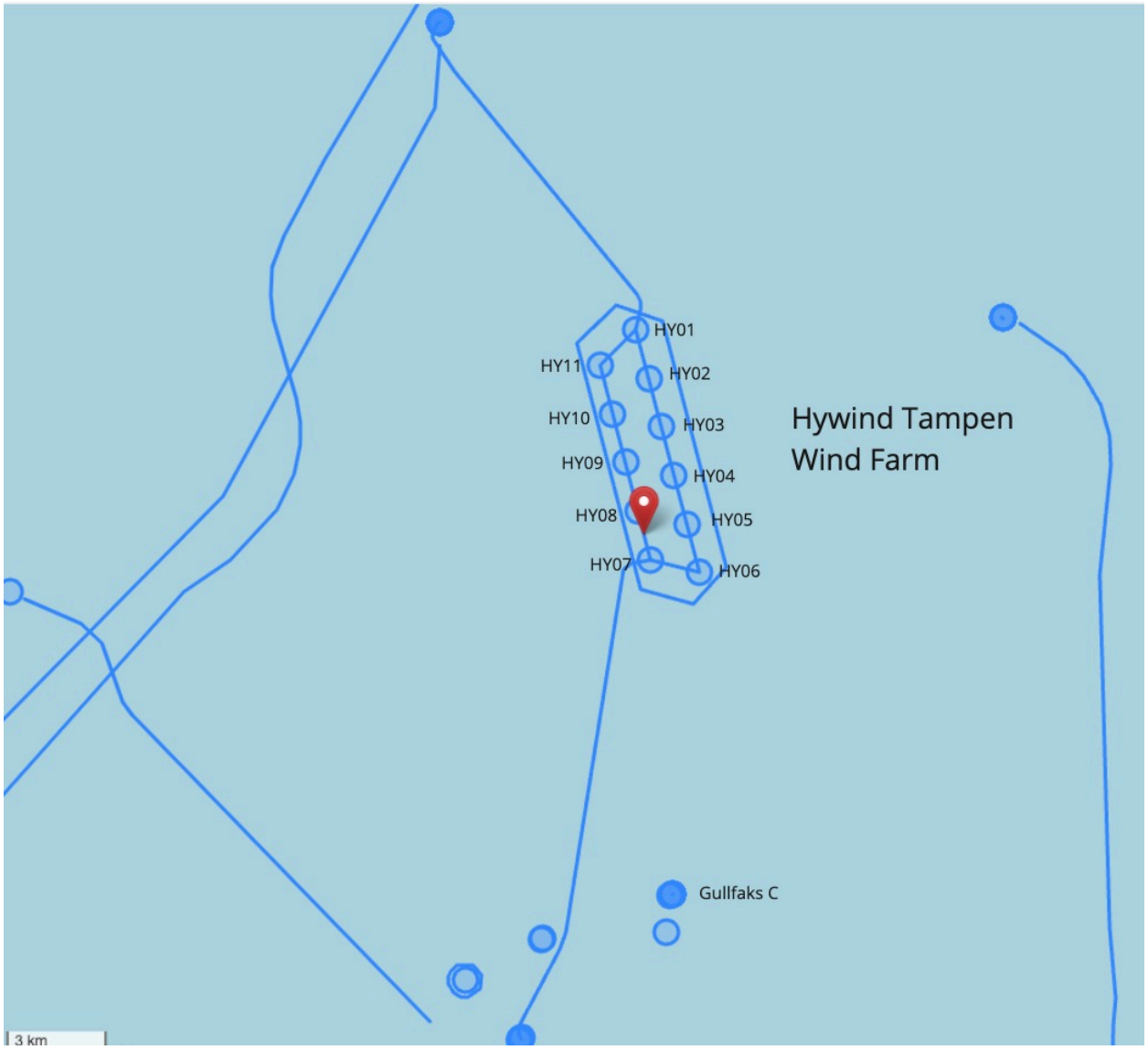

Figure 9: The position of the buoy, from OpenStreetMap. The red arrow indicated the buoy location. The Gullfaks C oil platform is just south of the Hywind Tampen wind farm and the Snorre oil field is to the north.

Figure 10: The field of view of Camera 1, captured 27 June 2024 at 08:35 AM. The current orientation is westwards, away from the wind farm and out in the open sea. The red dots is a bird flight track superimposed on the image.

Figure 11: The field of view of Camera 2, captured 27 June 2024 at 08:35 AM. The current orientation is northwards through the wind farm. The green dots is a bird flight track superimposed on the image.

Figure 12: The field of view of Camera 3, captured 27 June 2023 at 08:35 AM. The current orientation is eastwards, through the wind farm. The green dots is a bird flight track superimposed on the image.

Figure 13: The field of view of Camera 4, captured 27 June 2023 at 08:35 AM. The current orientation is southwards towards the Gullfaks C oil field - the oil platforms are visible in the horizon. The green dots is a bird flight track superimposed on the image.

Results

Measurement period

The measurement period was originally planned for 9 months, starting January 2023. Due to adverse weather conditions, the deployment was delayed and the buoy was finally deployed in June 2023.

The first day of data capture was 10 June 2023, and the last day was 14 October 2023. The measurement period lasted 127 days; 4 months and 4 days. During the measurement period, there were no days without data being collected, as seen in Figure 14. The measurement period covered part of the summer (10 June - 31 July) and autumn (1 August - 14 October). A total of 4,880 hours of data was captured. On average, 38.4 hours of video were captured per day, equalling 9.6 hours per camera.

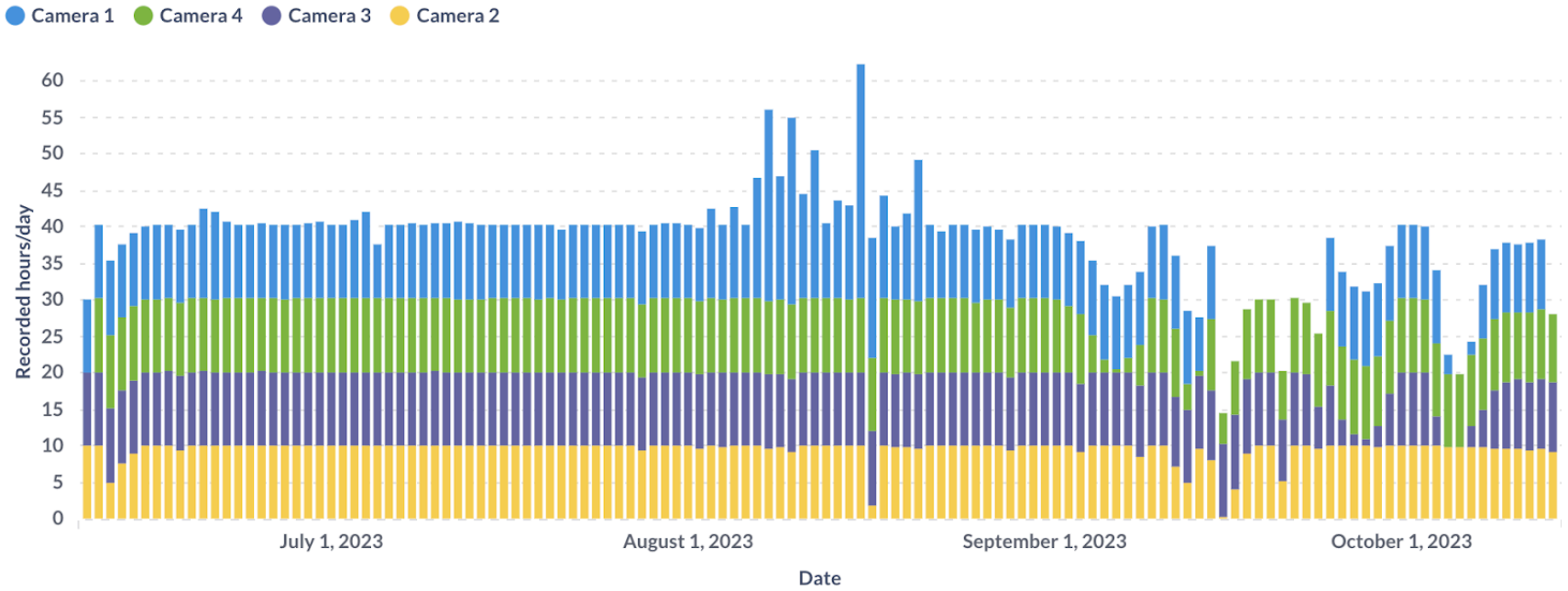

Figure 14: The hours of recording per day per camera, in the measurement period.

As seen in Figure 14, the number of recorded hours per day varies. Camera 1 did not record anything between 15 and 25 September. The number of recorded hours are found by multiplying the number of video files by 5 minutes, since the AXIS cameras by default record in 5 minute segments. The apparent increase of recorded hours in August is explained by some of the segments from Camera 1 being cut off at lower duration than 5 minutes. There is also a decrease of recorded hours in the middle of september. The power supply to the cameras has been controlled by Fugro and the difference in recorded hours is mainly explained by testing and shutting off cameras to save power.

The daily time period of data capture was scheduled to be between 06:00-16:00 UTC; 08:00-18:00 local time (UTC+2). The distribution of recorded hours during the day is shown in Figure 15.

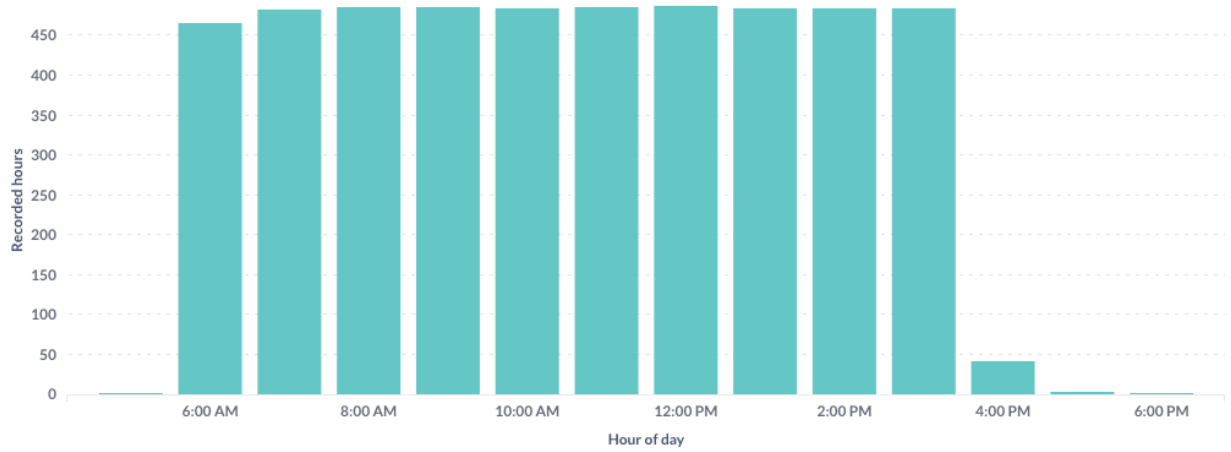

Figure 15: The total number of recorded hours for all cameras across the measurement period, per hour of day. As the recording was programmed to start and stop at fixed times, the distribution is relatively constant. Note the timestamp in UTC, corresponding to local time UTC+2.

Data capture

A total of 28 TB was captured during the 127 days, using almost 60% of the available 48 TB storage.

On average, this equals 220 GB per day, or 5.7 GB per hour. In other words, each camera captured on average 1.4 GB of data per operative hour.

Results by camera and camera types

2,482 hours were recorded for the dome cameras (Camera 1 and 2), and 2,399 hours were recorded for the bullet cameras (Camera 3 and 4), as seen in Table 3. Camera 1 lacks recordings for 9 full days from 16 - 24 September. A total of 26,258 birds were detected on the videos from the dome cameras, while 29,610 birds were detected on the bullet camera videos.

	Camera 1 Dome	Camera 2 Dome	Dome Total	Camera 3 Bullet	Camera 4 Bullet	Bullet Total
Recorded hours Assumes 5 min per video file	1,263 h	1,219 h	**2,482 h**	1,192 h	1,206 h	**2,398 h**
Detection count Number of bird detections	10,841	15,417	**26,258**	12,524	17,086	**29,610**
Average detection duration In seconds	3.6	3.5	**3.6**	3.1	3.3	**3.2**
Standard deviation of average detection duration	2.42	2.08	**2.23**	1.83	1.95	**1.90**
Detection rate Number of bird detections per recorded hour	8.6	12.6	**10.6**	10.6	14.2	**12.3**
Bird hours Total duration of all unique bird detections	10.9 h	15.0 h	**25.9 h**	10.7 h	15.5 h	**26.2 h**
Days with no recording	11	0	**11**	2	0	**2**

Table 3: Detection results for each camera, and per camera type, across the full measurement period.

The average duration of bird detections for the dome cameras (Camera 1 and 2) were 3.6 seconds, while for the bullet cameras (Camera 3 and 4) it was 3.2 seconds. That means that the duration of bird detections were on average 12% longer for the dome cameras compared to bullet cameras. The standard deviation for the detection durations were 2.23 seconds for the dome cameras (sample size of 26,258), and 1.90 seconds for the bullet cameras (sample size of 29.612).

Statistical testing shows that the differences in detections between the cameras and camera types are significant (Linear Mixed Effects model). In other words, the camera and camera type are significant predictors of detection rate ($p<0.001$) Furthermore from paired t-tests between each group, the mean for Camera 1 is significantly different from Camera 2 and 4 ($p<0.0001$) and the mean for Camera 3 is significantly different from 4 ($p<0.01$) The mean for Camera 1 is not significantly different from 3, and the mean for Camera 2 is not significantly different from 3 and 4.

As Camera 1 lacked recordings from 16 - 24 September, it motivates further investigation of the period. For the bullet cameras, 7,524 bird detections happened during these nine days alone, constituting 25% of the total bird detection count for the measurement period. The detection count for Camera 2 was 3,679 which constitutes 24% of the detections in the measurement period.

Table 3, and the statistical testing, shows a significant difference in detection count between Camera 3 and 4.The daily difference in detections is visualised in Figure 16. It is clear that the differences are distributed across the full measurement period.

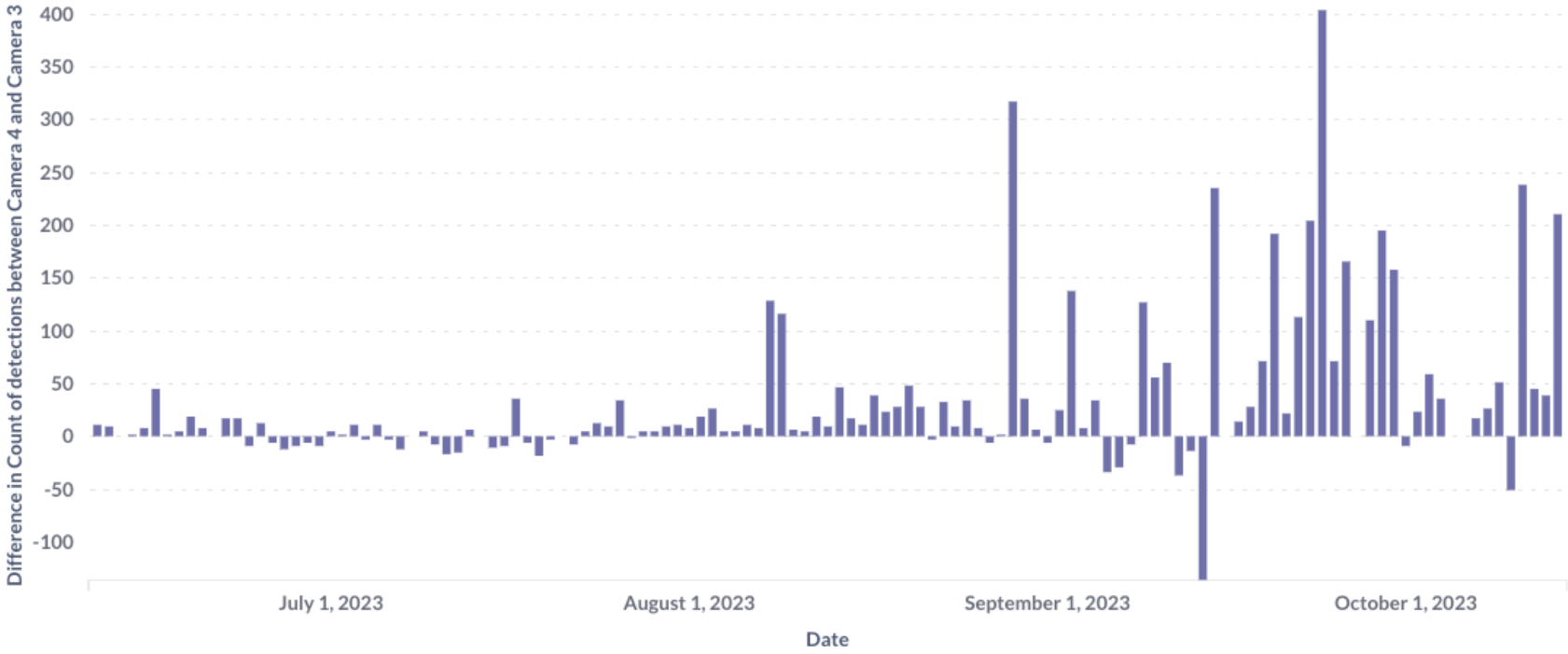

Figure 16: The difference in detection counts per day, between Camera 4 and Camera 3.

Fugro provided a datasheet showing the mean yaw (orientation) of the buoy with 10 minute resolutions. A rough analysis shows that the mean yaw had a northerly (316°– 45°) orientation 33% of the time, an easterly (46°– 135°) orientation 33% of the time, a southerly (136°– 225°) orientation 9% of the time and westerly (226°– 315°) orientation 25% of the time. This shows that although the buoy in theory could move freely, it more often had northwards and westwards orientations.

Data quality

A total of 78,709 detections were made by Spoor AI during the measurement period.

Out of all the detections, the average duration was 3.4 seconds and the median duration was 2.7 seconds. The maximum detection duration was 32.6 seconds, observed 14 June 2023.

90% of the detections had duration below 5.5 seconds, and the distribution is illustrated in Figure 17. No detections were below 1 seconds, as this is a lower threshold defined by Spoor.

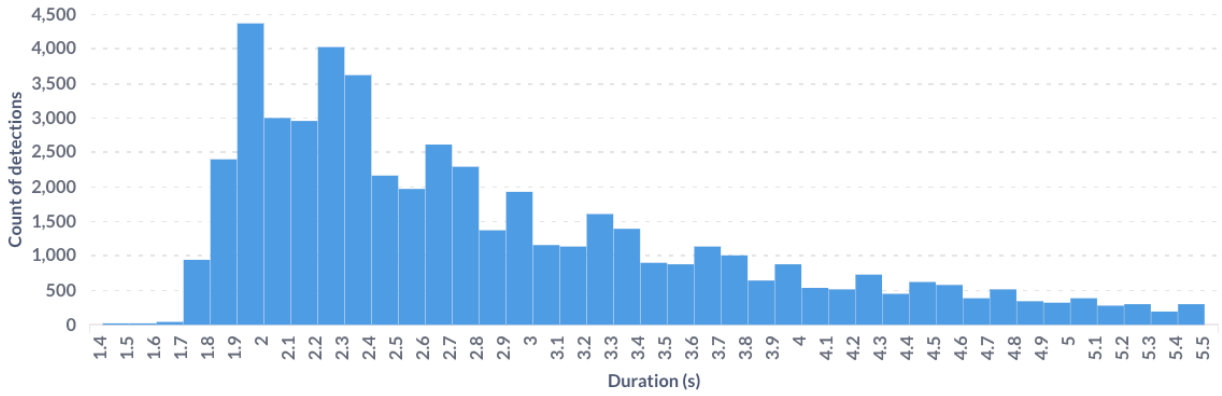

Figure 17: The distribution of bird detection durations, of detections within the 90 percentile of 5.5 seconds

Figure 18 shows the average duration per day for bird detections correlated with daily average wind speed, and it is clear that average duration declines with increasing wind speed. The trend plateaus at around 3 seconds.

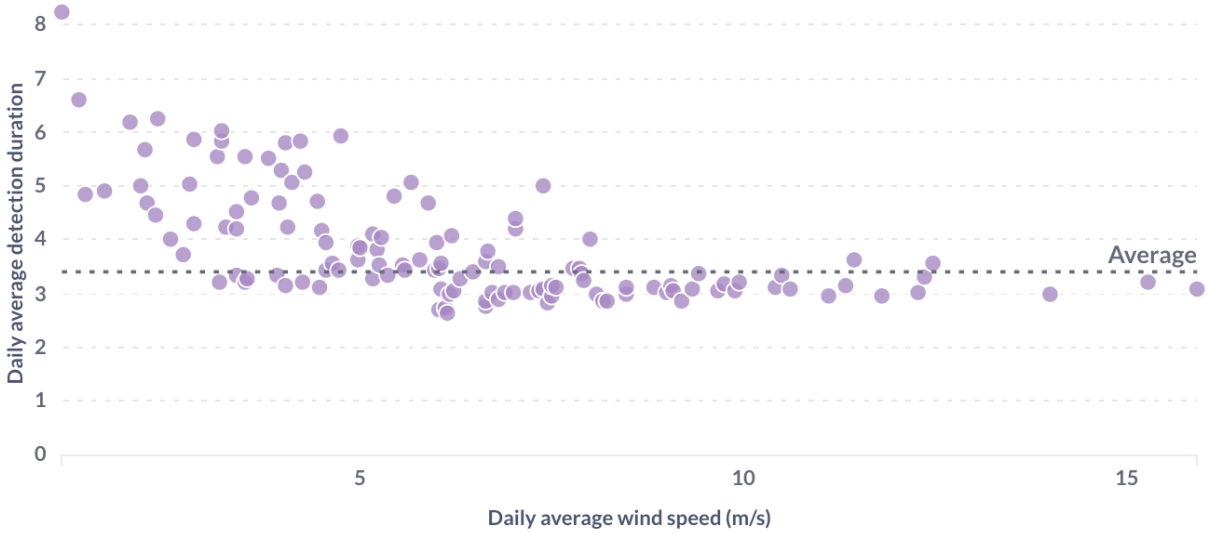

Figure 18: Daily average duration of bird detections correlated with daily average wind speed. The graph indicates that increased wind speed correlates with shorter detection duration.

To serve as a comparison, the same dimensions from the CCTV data, from *Pilot Report. Spoor - AI Avian Monitoring with CCTV Cameras on Floating Wind Turbines. Experiences and Future Potential* (2024), are plotted in Figure 19. It does not show the same clear correlation as in Figure 18.

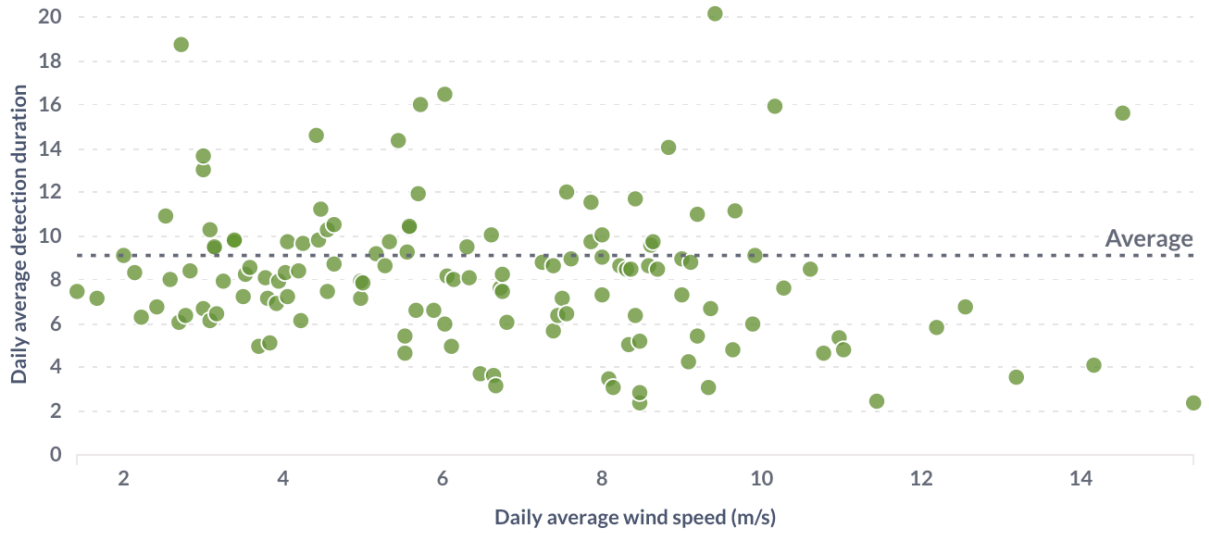

Figure 19: Daily average duration of bird detections, from Pilot Report. Spoor - AI Avian Monitoring with CCTV Cameras on Floating Wind Turbines. Experiences and Future Potential (2024)*, correlated with daily average wind speed. The graph indicates a less clear correlation between wind speed and detection duration.*

Bird activity

Activity throughout the measurement period

Count of detections

A total of 55,868 bird detections were registered for the four cameras across the full measurement period, with an average of 240 daily detections, a median of 210 daily detections and a standard deviation of 651 (sample size 127 days).

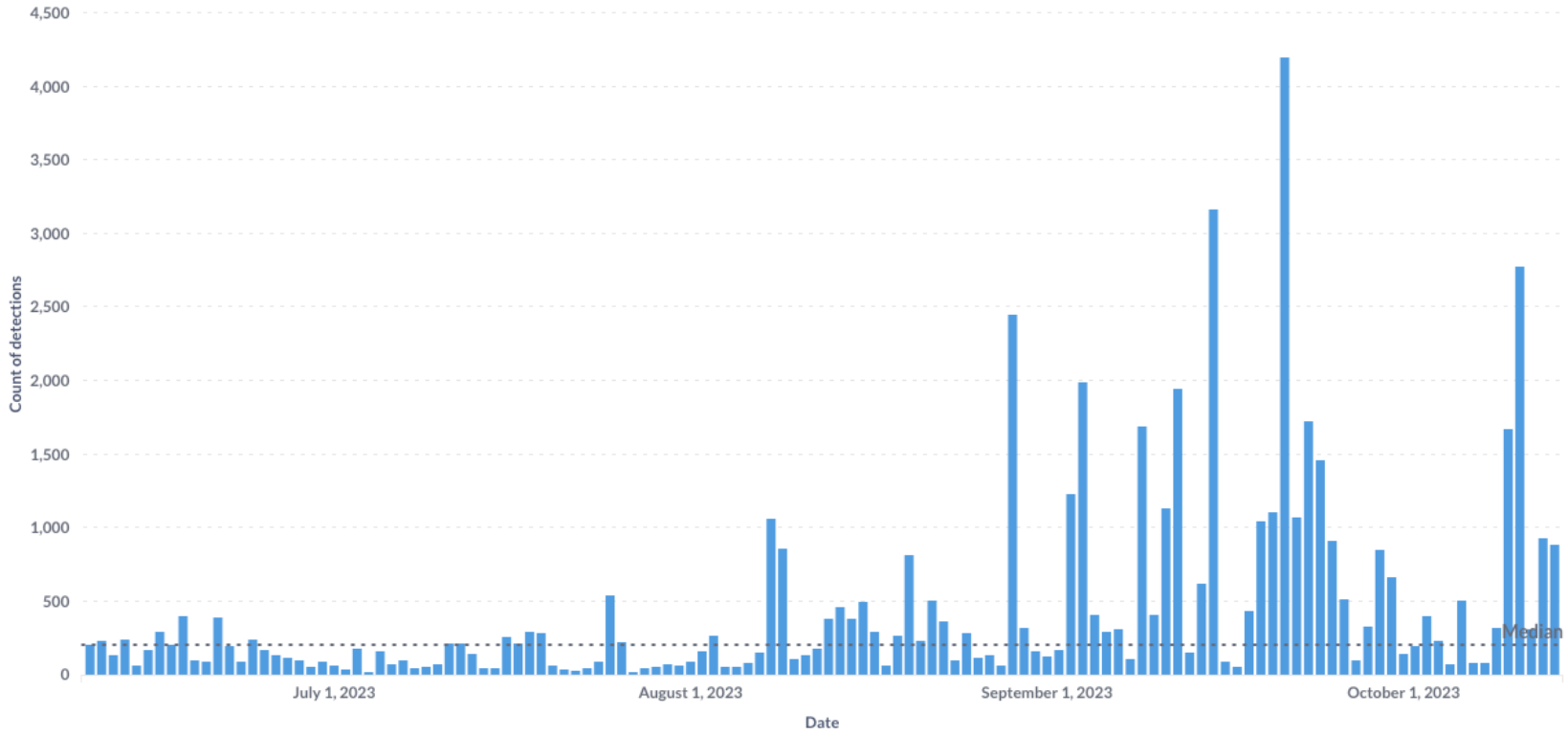

Figure 20: Absolute count of birds detected throughout the measurement period for all cameras. The median number of detections per day was 210, indicated by a black dotted line. Periods of low activity are seen in June and July, and increases from late August throughout September. The peak is 21 September

Detection rates

The absolute count of detections can be affected by any difference in the number of recorded hours per day. The number of recorded hours are shown in Figure 14. By dividing the daily count of detections by the number of recorded hours for that day, we get *detection rate* measured as the number of bird detections per hour of recording. The daily detection rates are displayed in Figure 21.

The overall detection rate for the full measurement period was 11.4 bird detections per recorded hour. The daily average was 12.9 detections/hour and the median was 5.2 detections/hour.

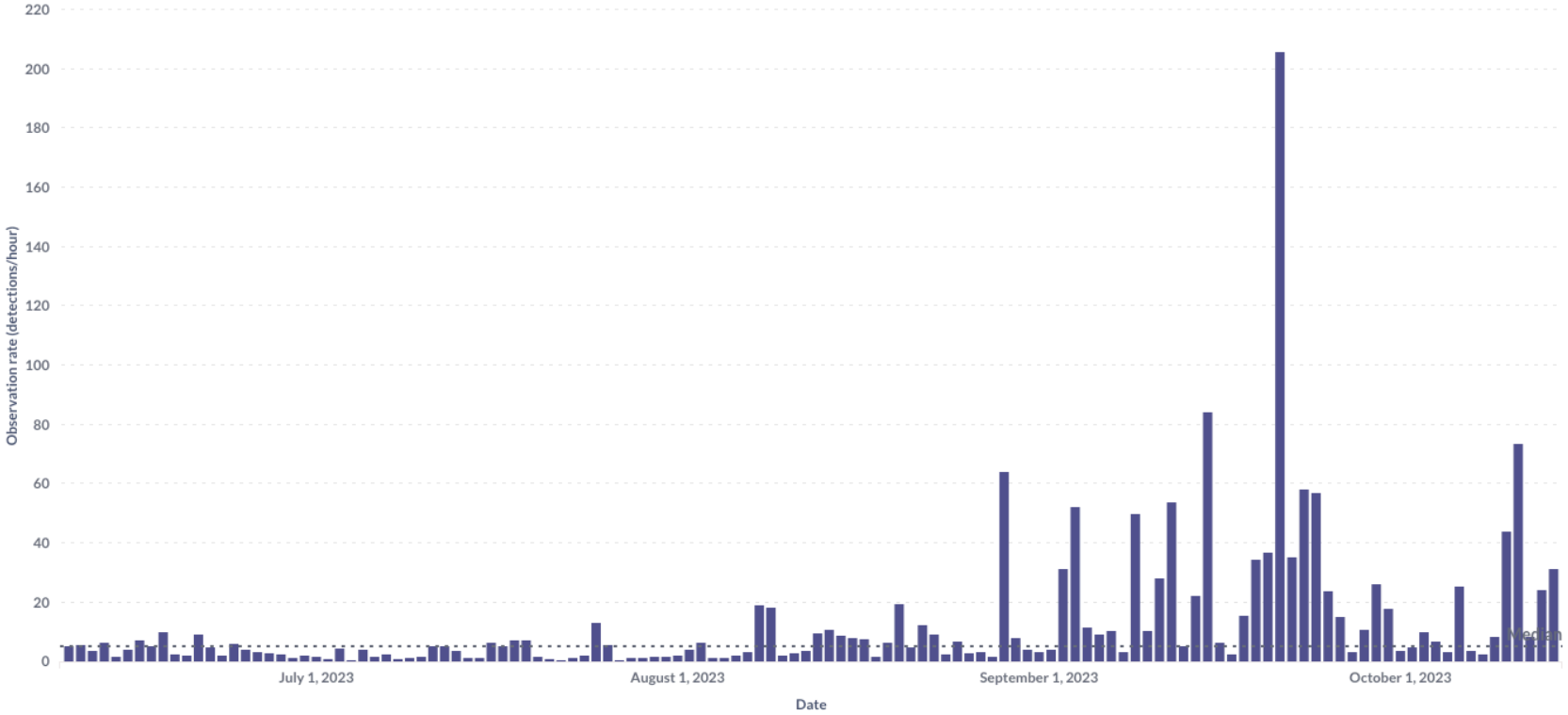

Figure 21: The daily detection rates (bird detections/recorded hour). The median detection rate of 5.2 is visualised by a black dotted line. The first significant peak day of activity was 29 August, and the absolute peak was 21 September.

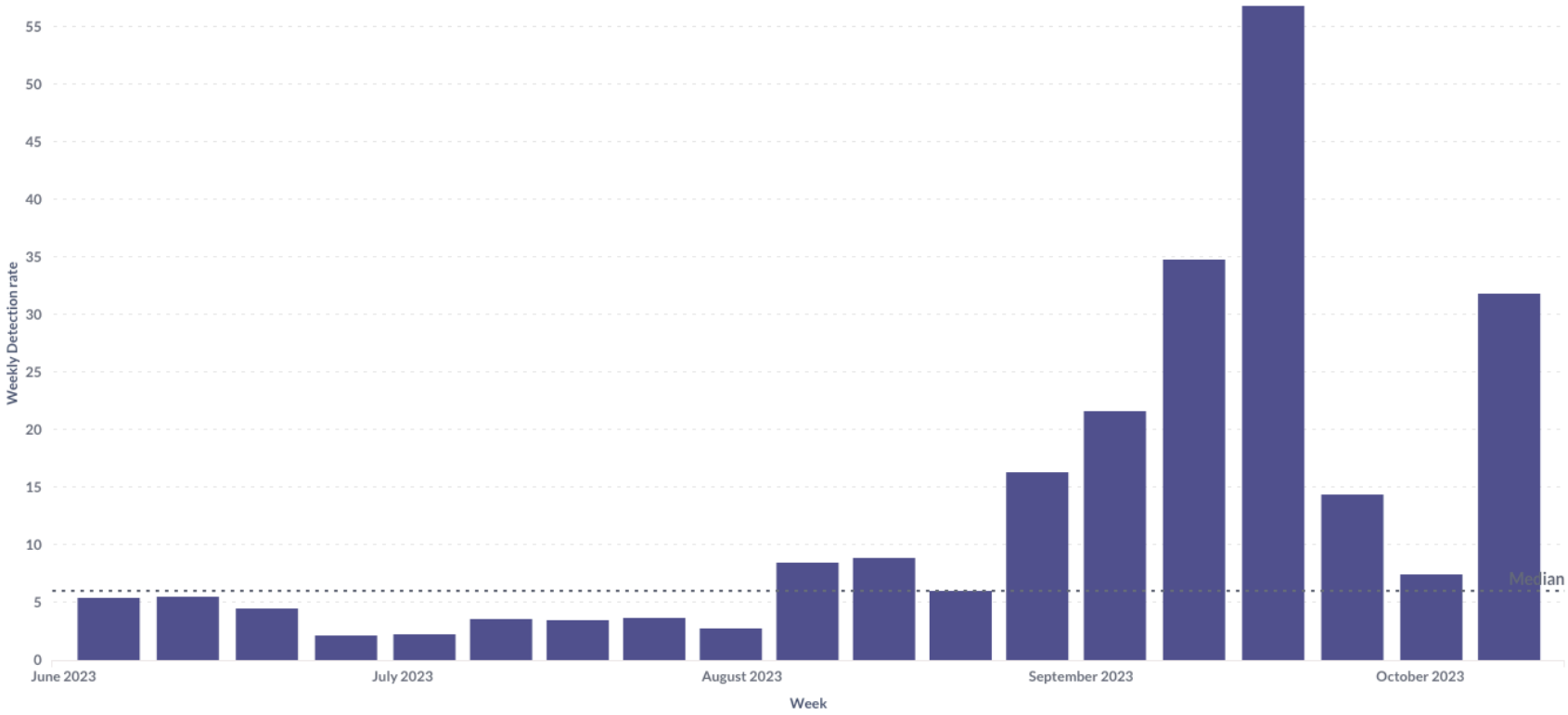

Figure 22: The weekly detection rates make the trends more expressed. The week of 7-13 August shows the first value above the median for the period. The peak is the week of 18-24 September.

The average weekly detection rate was 12.65 detections/hour, and the median was 6.1 detections/hour, as shown in Figure 22. The standard deviation was 14.0 (sample size 19 weeks). A slight increase above the median value was seen in the week of 7-13 August, indicating the start of a period of higher activity.

The detection rates per time of day is shown as box plots in Figure 23. The median values are indicated by the horizontal black line in the purple boxes, and are around 5 detections/hour for all operating hours of the day. The purple boxes represent 50% of the values, and the upper and lower lines represent the other 90% of the values. Outlier values are indicated by circles. Note that recordings were scheduled for 6AM - 4PM UTC. Recordings from outside these time slots have not been included in Figure 23.

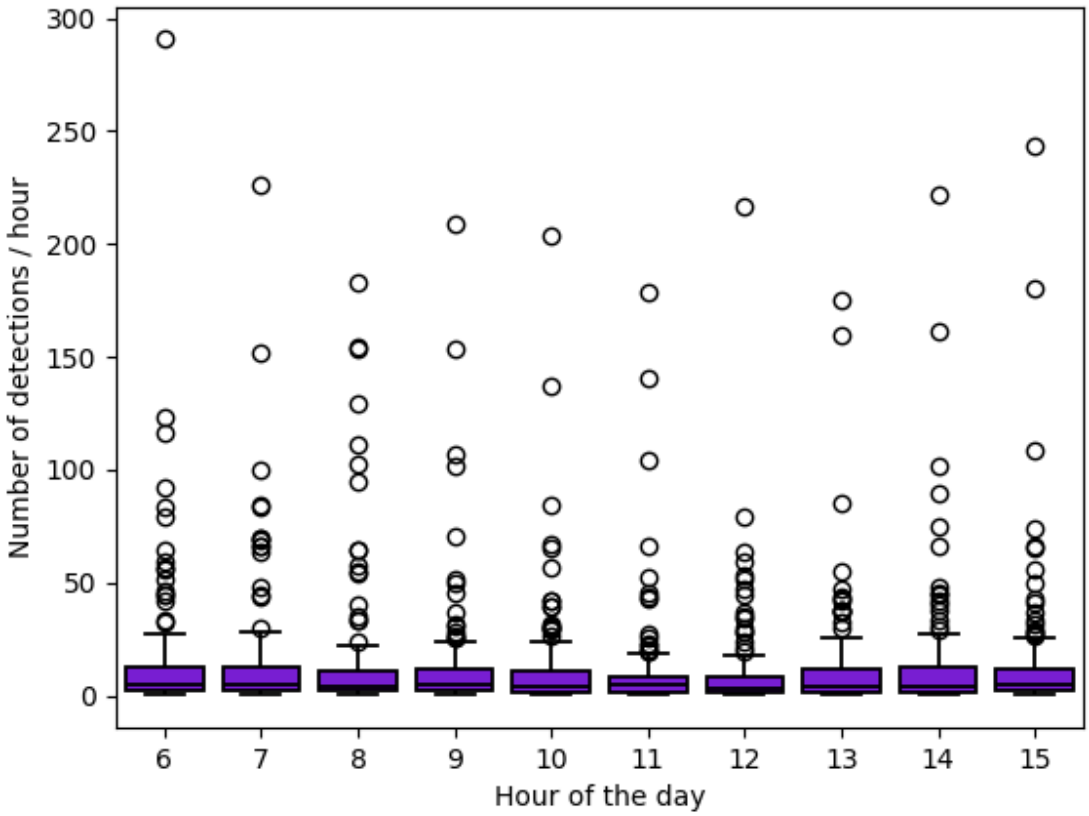

Figure 23: The detection rates per hour of day. The median values are around 5 detections/hour for all operating hours of the day. Recordings were scheduled mainly between 6AM-4PM UTC. Note the timestamp in UTC, while local time was UTC+2.

The outlier values seen in Figure 23 indicates that it is a heavy-tailed distribution, which is characterised by a large probability of observing large deviations from the mean (outliers). This means that bird activity from day to day is so varied that it cannot be fully understood by simply averaging over time.

Bird minutes

Bird minutes is defined as the total duration of unique bird detections. Figure 24 shows the timeline for bird minutes per day for the four cameras. A total of 3,126.4 bird minutes were registered for the full measurement period, equal to 52.1 hours. The average was 24.6 minutes per day and the median was 11 minutes per day.

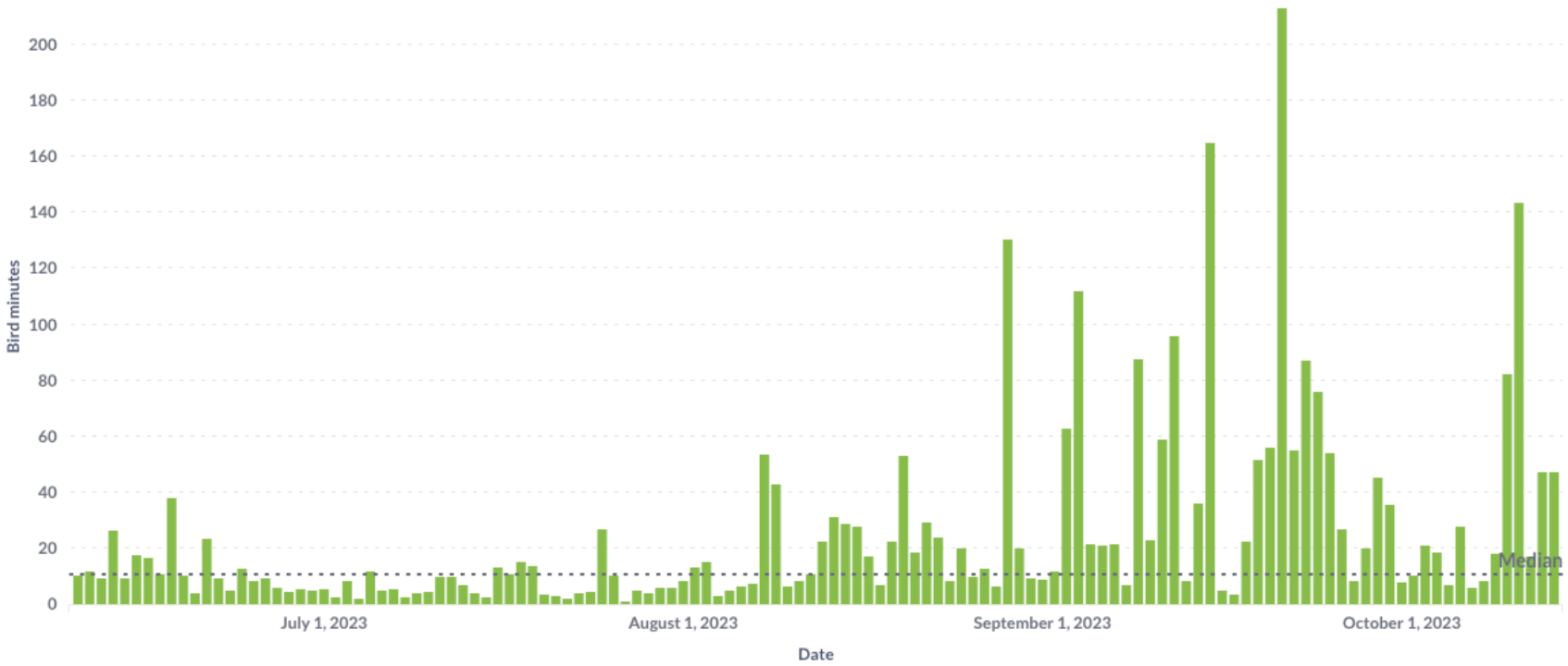

Figure 24: The bird minutes per day for the measurement period. The median value of 11 is indicated by the dotted line.

Bird minute rate

Bird minute rate takes into account the duration of recording, and is defined as the total duration of unique bird detections per recorded minute. The resulting value is multiplied by 100 for readability. Figure 25 shows the timeline for bird minute rates for the four cameras. The daily average was 1.19, and the median was 0.50.

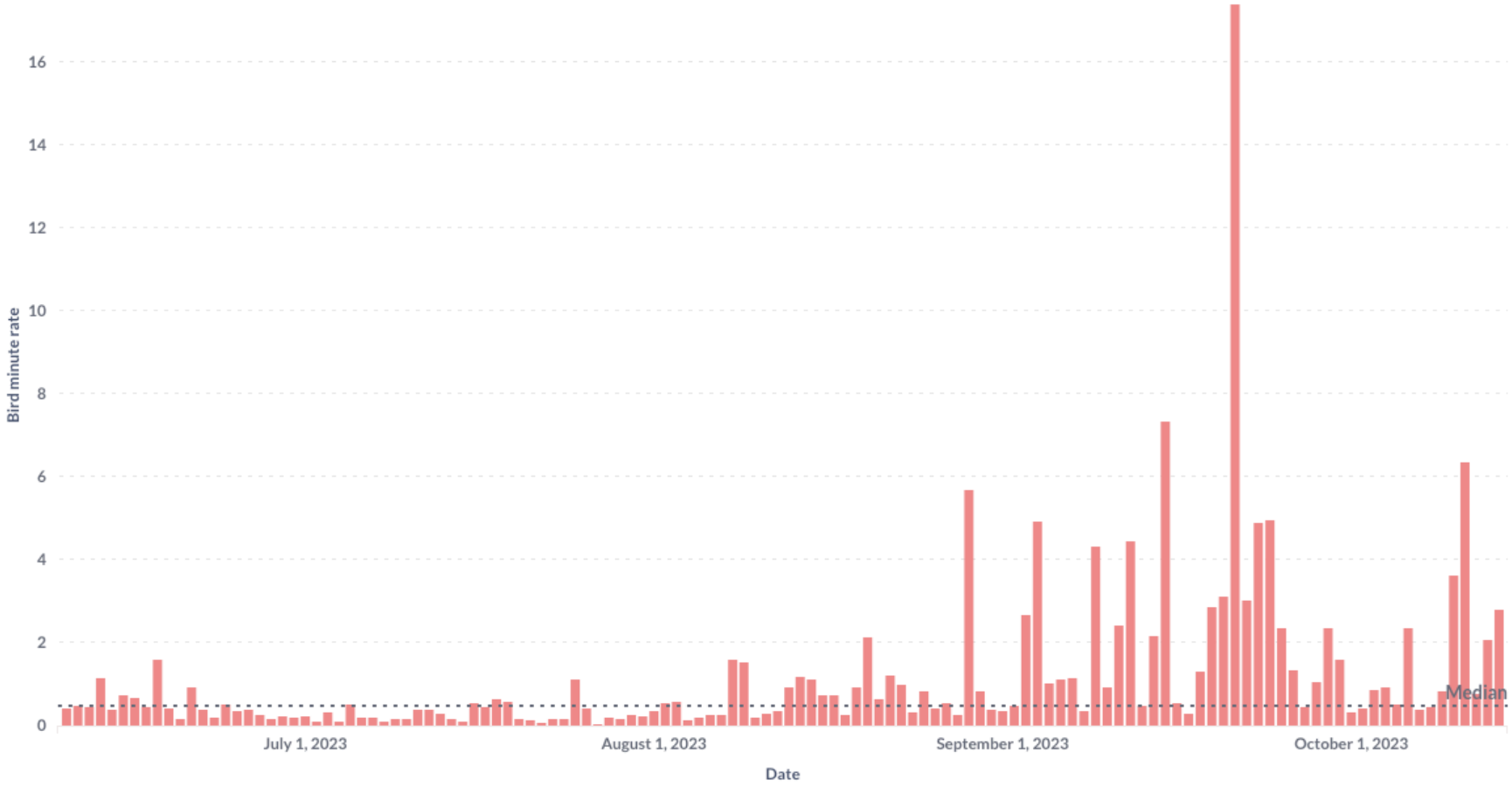

Figure 25: Daily bird minute rates throughout the measurement period for all cameras. The daily median of 0.50 is indicated by a black dotted line. Periods of low activity are seen in June and July, and increases from late August throughout September. The peak is 21 September.

Weekly bird minute rate is shown in Figure 26. Average weekly bird minute rates was 1.16 and median was 0.75, with a standard deviation of 1.18 (sample size 19 weeks). An increase starts in the week 7 - 13 August and peaks in the week 18 - 24 September.

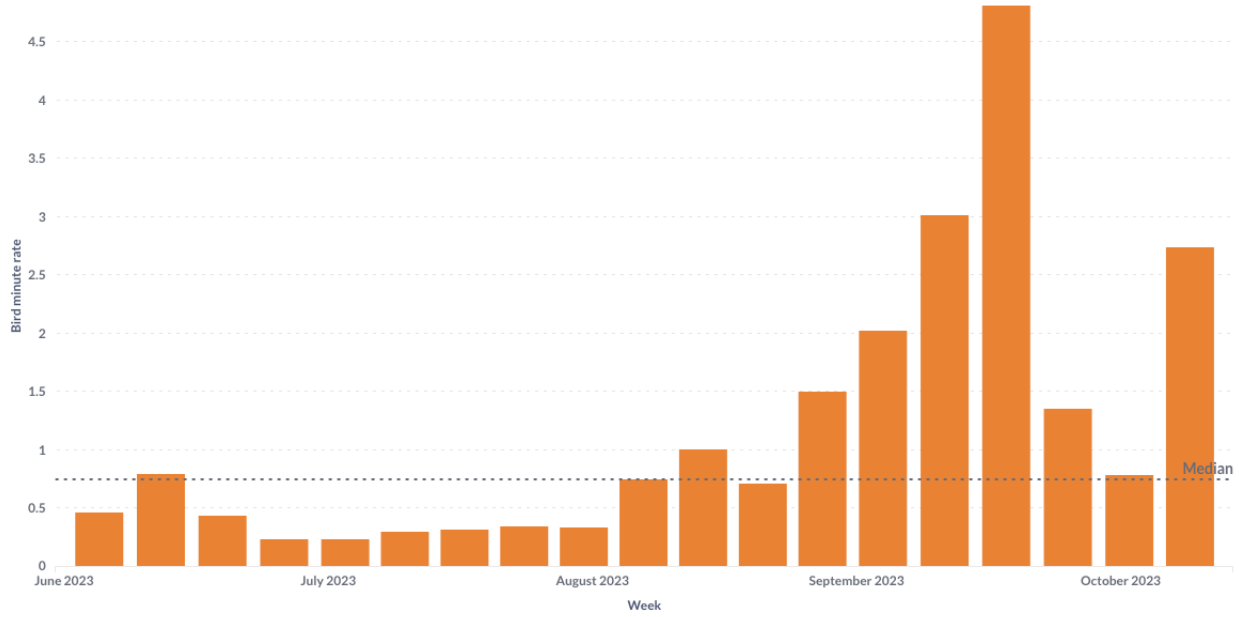

Figure 26: Weekly bird minute rates throughout the measurement period for all cameras. The first week above the median of 0.75 was the week of 12-18 June. The peak is in the week of 18 - 24 September.

Activity and weather conditions

The weather conditions in the measurement period have seen winds up to 24 m/s wind speed (registered 14 October 2023). The maximum daily precipitation was 26.4 mm (registered 8 August 2023). During the measurement period, the buoy experienced average wave heights of 6 m and maximum wave heights of 11 m.

Does bird activity correlate with wind direction? Figure 27 shows a scatter plot with daily detection rates (bird detections/recorded hour) and daily average wind direction, measured in degrees (0° is wind from north). Southerly and south-westerly winds correlate with higher detection rates.

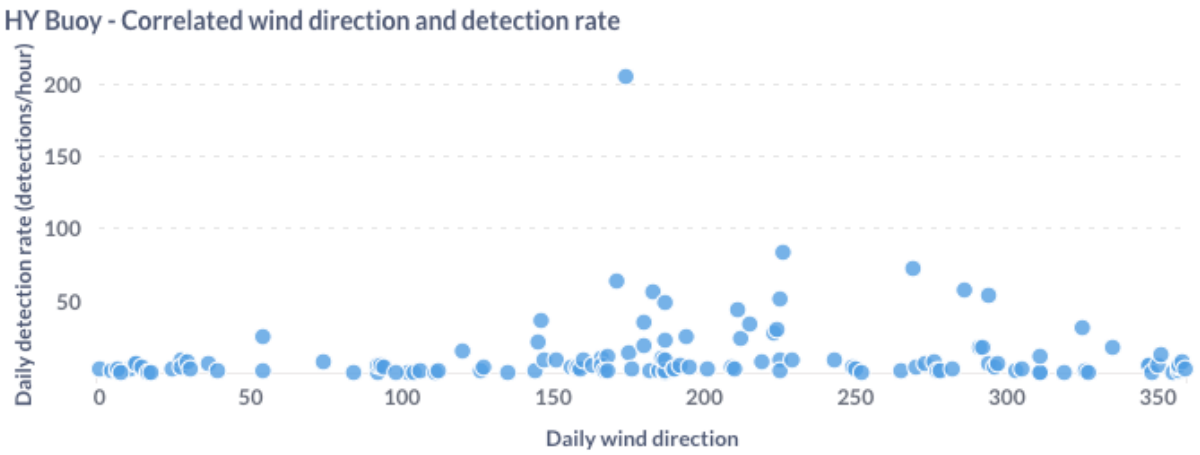

Figure 27: A scatter plot of the daily average wind direction (measured in degrees, where north is 0° and south is 180°) and the daily detection rates.

Table 4 shows a more granular picture with the wind direction averaged per hour instead of per day. The number of recorded hours per hourly wind direction, bird detections and detection rate for the measurement period is calculated. It repeats the result indicated in Figure 27; that higher bird activity correlates with southerly and westerly winds.

	Northerly winds 316°– 45°	Easterly winds 46°– 135°	Southerly winds 136°– 225°	Westerly winds 226°– 315°
Recorded hours	1,400	761	1,619	1,060
Bird detections	9,192	5,022	25,945	15,713
Detection rate Detections per analysed hour	6.6	6.6	16.0	14.8

Table 4: The detection rates when winds are blowing from North, East, South and West. The wind speed is averaged per hour, instead of per day as was the case in Figure 27. The highest detection rate was for Southerly winds.

In the measurement period, 34 days had average wind direction from north (316°– 45°), 18 days from east (46°– 135°), 49 days from south (136°– 225°) and 26 days from west (226°– 315°). The average wind speed for the days dominated by northerly winds was 5.5 m/s, while it was 4.5 m/s for easterly winds, 7.0 for southerly winds and 6.9 m/s for westerly winds.

Flight heights

A normalised flight height distribution across all four cameras are displayed in Figure 28. The highest density is observed in the 0-5 metre and the 5-10 metre height bins. The densities become negligible above 60 metres.

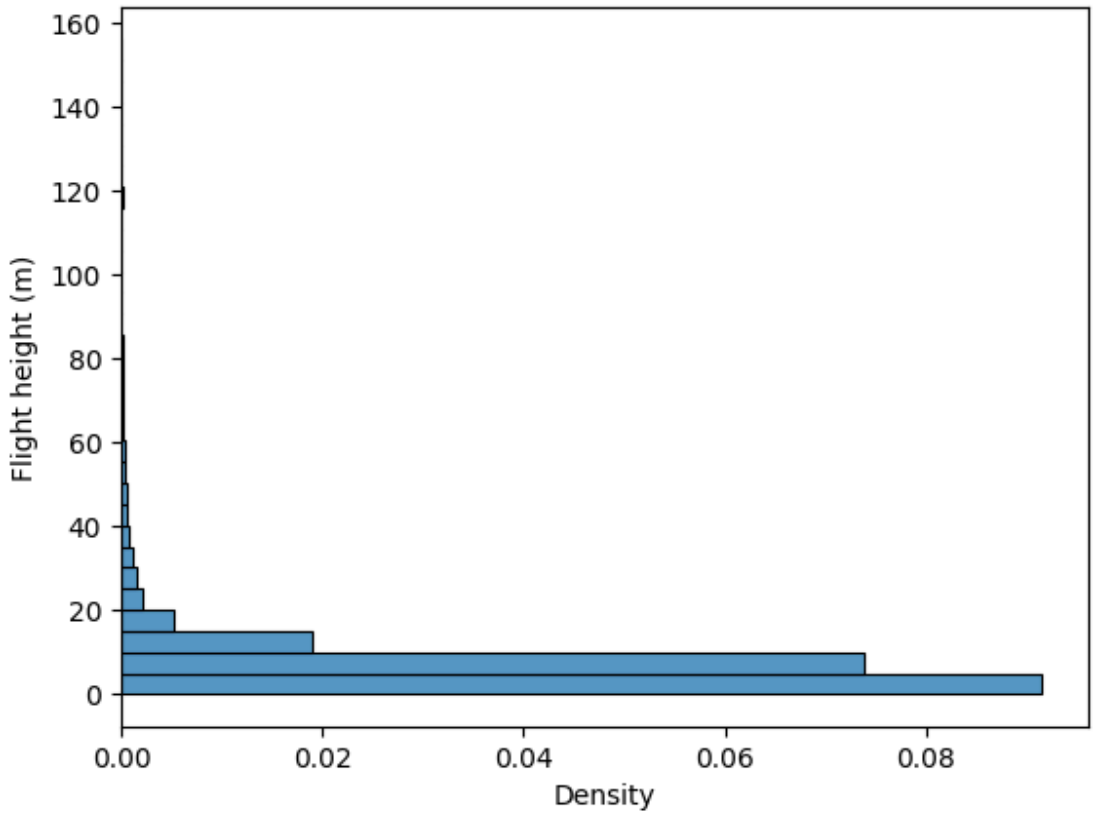

Figure 28: The unitless normalised flight height distribution (density) for all cameras. The highest density was measured in the height interval of 0-5 metres. Above 60 metres, the densities are negligible.

Figure 29 shows the flight height densities for the dome cameras Camera 1 and 2, respectively. The peak density is seen in the height bin 5-10 metres for both cameras, and the majority is from 0-15 metres.

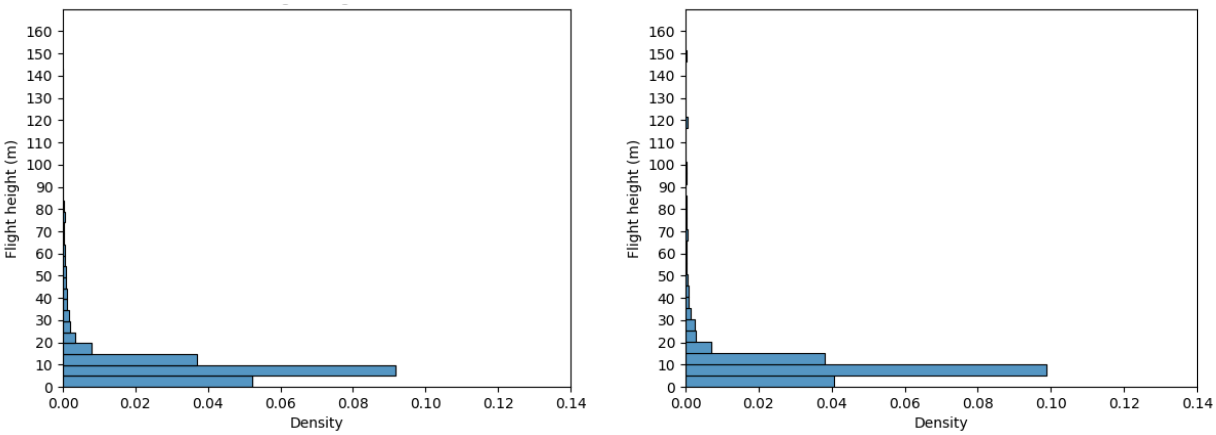

Figure 29: The flight height densities for Camera 1 (left) and Camera 2 (right). The highest densities were measured in the 5-10 metre height bins for both cameras.

Figure 30 shows the flight height densities for the bullet cameras Camera 3 and 4, respectively. The peak density is seen in the height bin 0-5 metres for both cameras, and the majority is within 0-10 metres.

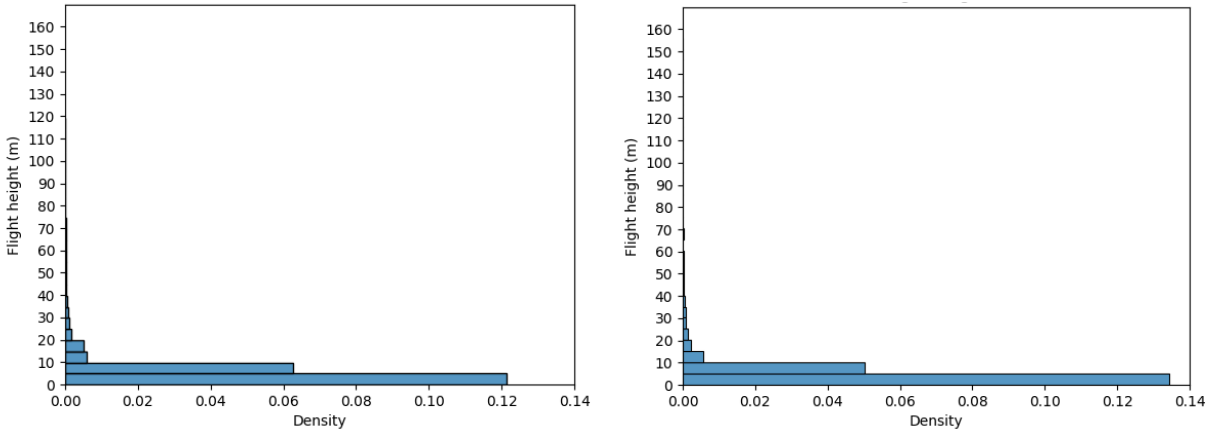

Figure 30: The flight height densities for Camera 3 (left) and Camera 4 (right). The highest densities were measured in the 0-5 metre height bins for both cameras.

Monthly activity

A monthly breakdown of recorded hours, bird detections, detection rate, bird minutes and bird minute rates, is shown in Table 5. The lowest activity levels, as indicated by the detection rate and bird minute rates, were in July, followed by June and August. The highest activity levels were in September, followed by October.

Metric	June Summer	July Summer	August Autumn	September Autumn	October Autumn
Recorded hours	843 h	1,250 h	1,349 h	967 h	471 h
Bird detections	3,762	3,890	11,200	28,382	8,634
Bird minutes Duration of all unique bird detections in minutes	257 min	217 min	683 min	1,503 min	464 min
Detection rate Bird detections per recorded hour	4.5	3.1	8.3	29.3	18.3
Bird minute rate Minutes of bird detections per recorded minute, multiplied by 100	0.51	0.29	0.84	2.59	1.64

Table 5: The monthly recorded hours, bird detections, bird minutes, detection rates and bird minute rates. The highest activity levels were in September, followed by October.

Days of peak activity

Five peak activity days	Top #1	Top #2	Top #3	Top #4	Top #5
Detection count	4,204 21 September	3,162 15 September	2,781 11 October	2,450 29 August	1,992 4 September
Detection rate	206 21 September	84 15 September	74 11 October	64 29 August	58 23 September
Bird minutes	213.0 21 September	164.8 15 September	143.7 11 October	130.6 29 August	112.1 4 September
Bird minute rates	17.39 21 September	7.33 15 September	6.35 11 October	5.69 29 August	4.98 24 September

Table 6: The five days of most observed bird activity for each of the four activity metrics. 21 September was the day of most activity for all metrics.

As seen in Table 6, the top four peak days 21 September, 15 September, 11 October and 29 August are the same across the different metrics. The metrics that are corrected for recording duration (detection rate and bird minute rate) has the fifth peak day as 23 and 24 September, while the absolute metrics (detection count and bird minutes) show 4 September as the fifth highest day of activity. The top three peak days are explored in more detail in the next sub-chapters.

21 September

A manual inspection of the 4,204 bird detections on 21 September showed that the vast majority of birds were Northern Fulmars cruising past. Figure 31 shows the detection count per hour for the five days leading up to 21 September, and the peak at 21 September.

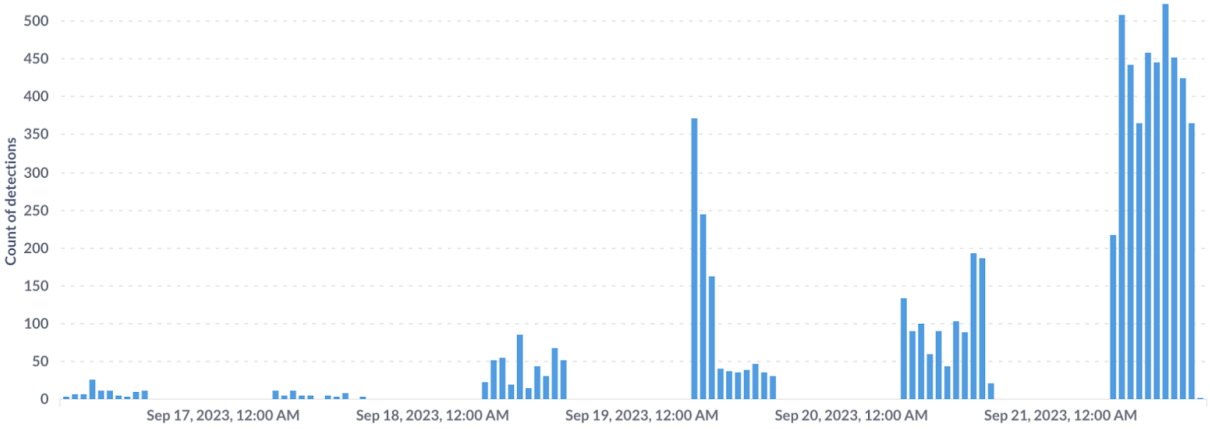

Figure 31: The detection count per hour, for the 21 September and the five days prior.

Table 7 shows the activity levels and weather conditions for the five days prior to the peak on 21 September. The change in bird activity from 20 to 21 September corresponds to a 560% increase in both detection rate and bird minute rate. The average wind direction in the prior days has not been calculated, as it gives little real insight. The daily average wind directions for the four days prior to 20 September were 347° (north), 106° (east), 120° (south-east), and 215° (south-west) in ascending order.

	Average 16-20 September	20 September	21 September
Wind speed	6.3 m/s	7.0 m/s	9.9 m/s
Wind direction	-	146° (south-east)	174° (south)
Precipitation	6.4 mm	14.1 mm	0
Detection rate	19.2	36.9	205.9
Bird minute rate	1.63	3.11	17.39

Table 7: The bird activity and weather conditions on the peak day 21 september, and the five days prior.

15 September

Figure 32 shows the detection count per hour for the five days leading up to 15 September, and the peak at 15 September.

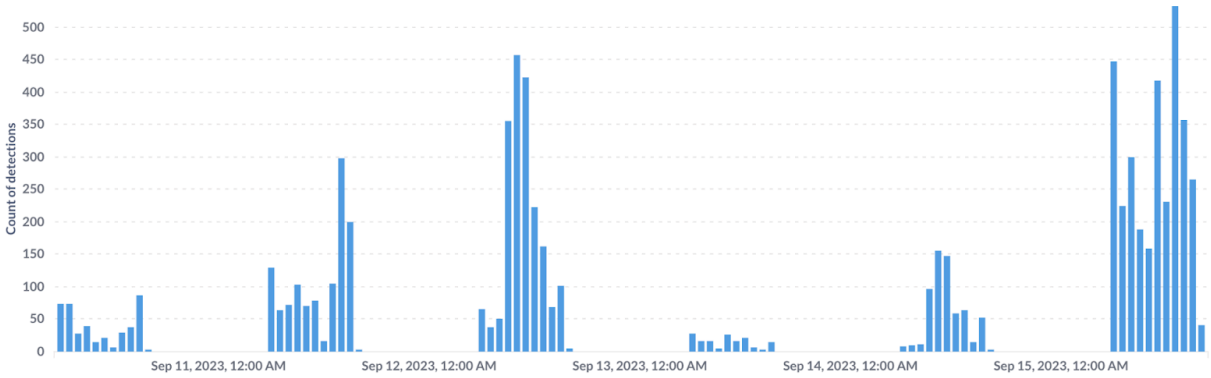

Figure 32: The detection count per hour, for the 15 September and the five days prior.

Table 8 shows the weather conditions and bird activity of the five days prior to the second highest peak day 15 September. The change in bird activity from 14 to 15 September corresponds to a 375% increase for detection rate and a 337% increase for bird minute rate. The daily average wind directions for the four days prior to 14 September were 229° (south-west), 223° (south-west), 294° (north-west), and 350° (north) in ascending order.

	Average 10-14 September	14 September	15 September
Wind speed	5.6 m/s	6.0 m/s	10.4 m/s
Wind direction	-	145°(south-east)	226°(south-west)
Precipitation	4.4 mm	2 mm	0 mm
Detection rate	24.1	22.4	84
Bird minute rate	2.97	2.17	7.33

Table 8: The bird activity and weather conditions on the second highest peak day; 15 September, and the five days prior.

11 October

This day had the highest average wind speed of all the days in the measurement period, and Figure 34 shows a Northern Fulmar navigating the strong winds. Figure 33 shows the detection count per hour for the five days leading up to 11 October, and the peak at 11 October.

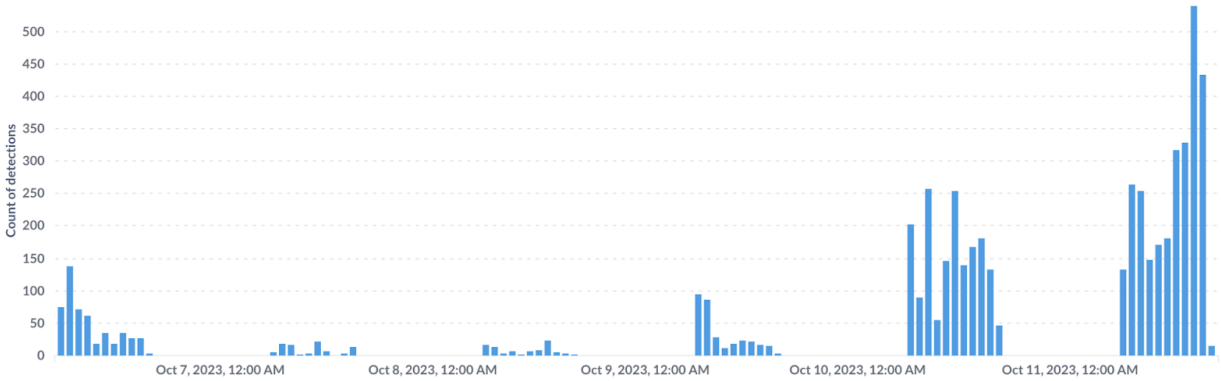

Figure 33: The detection count per hour, for the 11 October and the five days prior.

Table 9 shows the weather conditions and bird activity of the five days prior to the third highest peak day 11 October. The change in bird activity from 10 to 11 October corresponds to a ~170% increase for both detection rate and bird minute rate. The daily average wind directions for the four days prior to 10 October were 54° (north-east), 359° (north), 278° (west) and 219° (south-west) in ascending order.

	Average 6-10 October	10 October	11 October
Wind speed	7.5 m/s	11.1 m/s	15.9 m/s

	Average 6-10 October	10 October	11 October
Wind direction	-	211° (south-west)	269° (west)
Precipitation	7.5 mm	11.5 mm	6.1 mm
Detection rate	16.9	44.1	73.7
Bird minute rate	1.53	3.63	6.35

Table 9: The bird activity and weather conditions on the third highest peak day; 11 October, and the five days prior.

Figure 34: A Northern Fulmar navigating the strong winds 11 October 2023. This day had the highest average daily wind speed for the measurement period.

Days of lowest activity

All the five days of lowest activity were found during July, as seen in Table 10. The wind speed in July was on average 5.37 m/s and average precipitation per day was 1.83 mm. Around half of the days in July had northerly winds (including north-east and north-west). Only 3 days had westerly winds. The rest of the days had winds from south and east.

Five lowest activity days	Bottom #1	Bottom #2	Bottom #3	Bottom #4	Bottom #5
Detection count	19 27 July	26 4 July	31 22 July	39 21 July	43 2 July
Detection rate	0.47 27 July	0.62 4 July	0.77 22 July	0.99 21 July	1.07 2 July
Bird minutes	1.0 27 July	2.0 22 July	2.4 4 July	2.7 8 July	3.1 2 July
Bird minute rates	0.04 27 July	0.08 22 July	0.09 4 July	0.11 8 July	0.11 2 July

Table 10: The five days of the lowest measured activity during the measurement period. All the dates are in the month of July.

27 July was the day of lowest activity in the measurement period, across all metrics. Figure 35 shows the detection count per hour for the five days leading up to 27 July, including 27 July. The average wind speed this day was 3.2 m/s, a 17° wind direction corresponding to a northerly wind, and no precipitation.

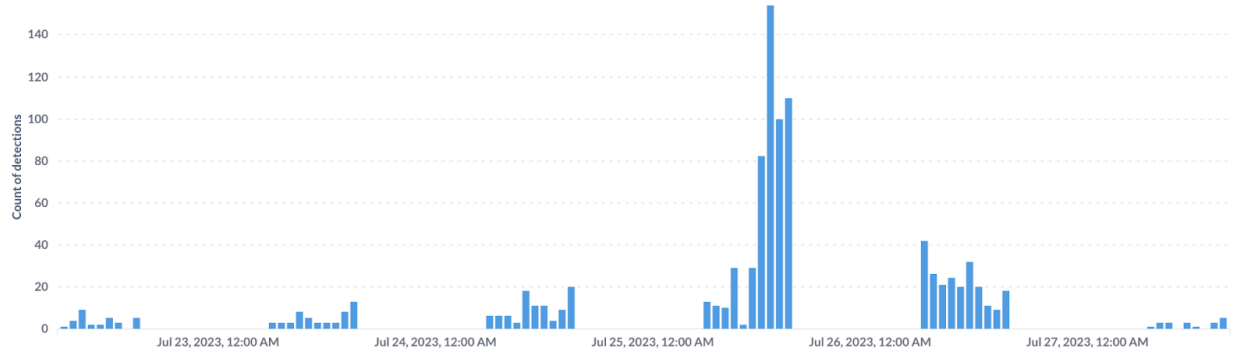

Figure 35: The detection count per hour, for the 27 July and the five days prior.

4 July and 22 July was the second and third least active day, interchangeably for the detection-based metrics and the bird minute-based metrics. 4 July had wind speed of 3.5 m/s, wind direction of 311° (north-east) and no precipitation. 22 July had a daily average wind speed of 5 m/s, a northerly wind direction of 16° and no precipitation.

The peak day of activity in July was 25 July – two days before the all-time lowest activity day of 27 July, also seen in Figure 35 – with a northerly wind speed of 8.5 m/s, 13.5 mm precipitation and a detection rate of 13.4.

Species

Figure 36: A Northern Fulmar captured 21 September 2023.

A sample of 2,068 bird detections – 4% of all the 55,868 detections – has been subject to taxonomic classification, with the following results:

- 1,534 (74%) could be classified to species level
- 1,656 (80%) could be classified to order, family or species level

That means that 412 detections (20%) could only be classified as “bird”.

As seen in Table 11, birds within five different orders and of five different species were identified. The black-legged kittiwake, seen in Figure 37, has Norwegian red list status endangered, and the European herring gull has status vulnerable, according to *Artsdatabanken: Norsk rødliste for arter 2021 (2021).* The other species do not have a protected status. The Northern Fulmar, shown in Figure 36, was the most detected species.

Classification *Order, family, subgroup, species*	Count *per level*	Red list status*
Charadriiformes; Shorebirds		-
- Gulls and Terns (Laridae)	114	-
Terns	4	-
Great Black-backed Gull (*Larus marinus*)	127	LC
Black-legged Kittiwake (*Rissa tridactyla*)	1	EN
European Herring Gull (*Larus argentatus*)	10	VU
- Alcidae - Common Murre / Razorbill	2	-
Suliformes		-
- Boobies and Gannets		-
Northern Gannet (*Morus bassanus*)	61	LC
Gaviiformes		-
- Loons	1	-
Procellariiformes		-
- Shearwaters and Petrels		-
Northern Fulmar (*Fulmarus glacialis*)	1,335	LC
Passeriformes; Passerines	1	-

Table 11: The count of observed birds per order, family and species level.
**LC = Least Concern, VU = Vulnerable, EN = Endangered*

The status after classifying ~1,500 detections was a distribution of 79% Northern Fulmars, 9% Great Black-backed Gulls, 7% Gulls (unspecified), 4% Northern Gannets, and four Terns, one Passerine, and one Common Murre/Razorbill.

After classifying the next 500 detections, one Loon and one Black-legged Kittiwake was found. The relative distribution between the rest of the species was largely unchanged; 81% Northern Fulmars, 8% Great Black-backed Gulls, 7% Gulls (unspecified), and 4% Northern Gannets, as shown in Figure 38.

Figure 37: A black-legged kittiwake captured by Camera 2 on 12 October 2023

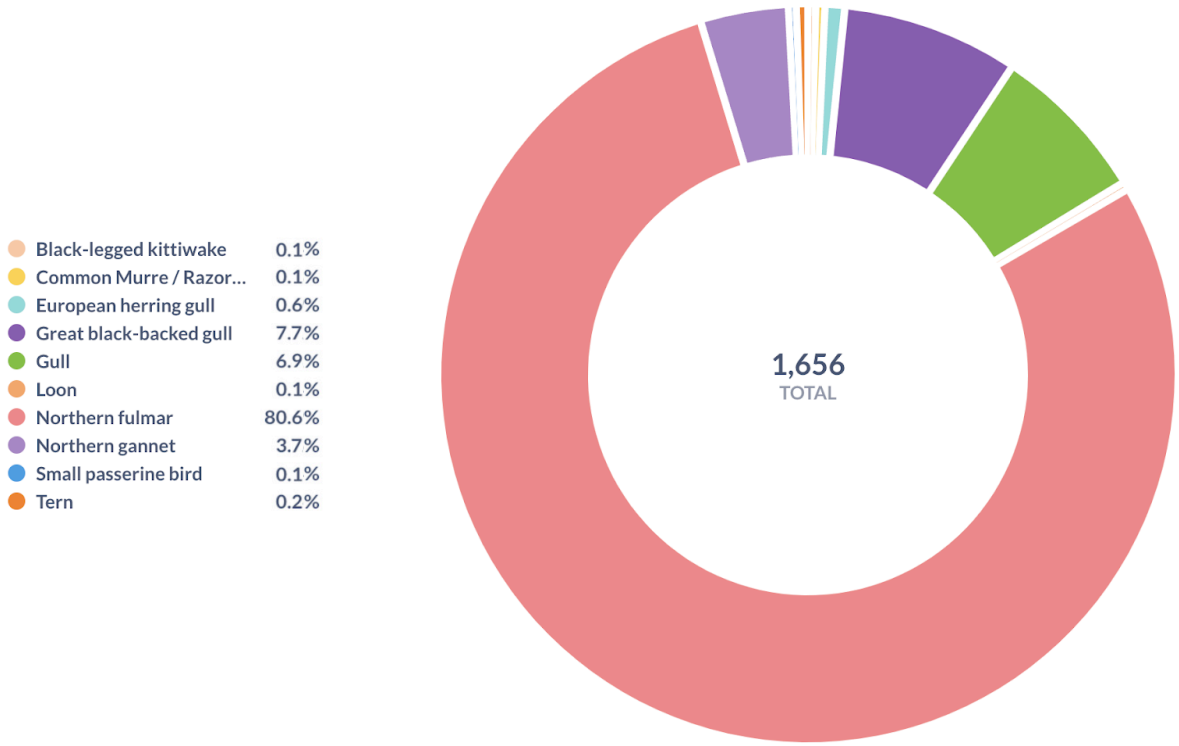

Figure 38: The distribution of bird classes for birds that could be classified on order, family or species level.

The monthly distribution of classified bird detections are shown in Table 12. The Great Black-backed Gull was the most detected species in June, while the Northern Fulmar was the most detected species in July - October. The European Herring Gull was only detected in June, while the Great Black-backed Gull, Northern Gannet and Northern Fulmars were detected in all months.

Class Order, family, species	June Summer	July Summer	August Autumn	September Autumn	October Autumn
Bird (unspecified)	93	68	103	113	30
Gull (unspecified)	49	15	23	14	9
European Herring Gull	10	-	-	-	-
Great Black-backed Gull	93	12	13	6	3
Black-Legged Kittiwake	-	-	-	-	1
Tern	-	-	3	1	-
Common Murre / Razorbill	1	1	-	-	-
Northern Gannet	10	22	14	1	1
Northern Fulmar	41	84	388	666	156
Small passerine bird	-	1	-	-	-
Loon	-	-	-	-	1

Table 12: The monthly distribution of number of bird detections, for detections that were subjected to taxonomic classification.

The share of each bird category per monthly sample is shown in Table 13. The Great Black-backed Gull was the species with the largest share of detections in June, while the Northern Fulmar was the species with the largest share of detections in July - October.

Class Order, family, species	June Summer	July Summer	August Autumn	September Autumn	October Autumn
Bird (unspecified)	31.3%	33.5%	18.9%	14.1%	14.9%
Gull (unspecified)	16.5%	7.4%	4.2%	1.7%	4.5%
European Herring Gull	3.4%	-	-	-	-
Great Black-Backed Gull	31.3%	5.9%	2.4%	0.7%	1.5%
Black-Legged Kittiwake	-	-	-	-	0.5%
Tern	-	-	0.6%	0.1%	-
Common Murre / Razorbill	0.4%	0.5%	-	-	-
Northern Gannet	3.4%	10.8%	2.6%	0.1%	0.5%
Northern Fulmar	13.8%	41.4%	71.3%	83.1%	77.6%
Small passerine bird	-	0.5%	-	-	-
Loon	-	-	-	-	0.5%

Table 13: The monthly relative distribution of bird detections that were subjected to taxonomic classification. The Northern Fulmar has an increased share from the summer to autumn, peaking in September where this species accounted for 83% of the sample.

Behaviour

Different types of bird behaviour have been observed throughout the measurement period; in particular resting, feeding, local movements by residential birds, and migration.

Figure 39 shows a gull that is approaching the buoy, likely about to land. The buoy provides an attractive resting ground for some birds. Birds have also been observed resting on the sea surface, like the Northern Fulmars in Figure 40.

Several examples of Northern Fulmars feeding on the ocean surface in front of the buoy have also been observed, as indicated by the active posture of several of the birds in Figure 40.

Figure 39: A gull approaching the buoy, captured 26 June 2023. The buoy can serve as a resting object and may thus attract birds.

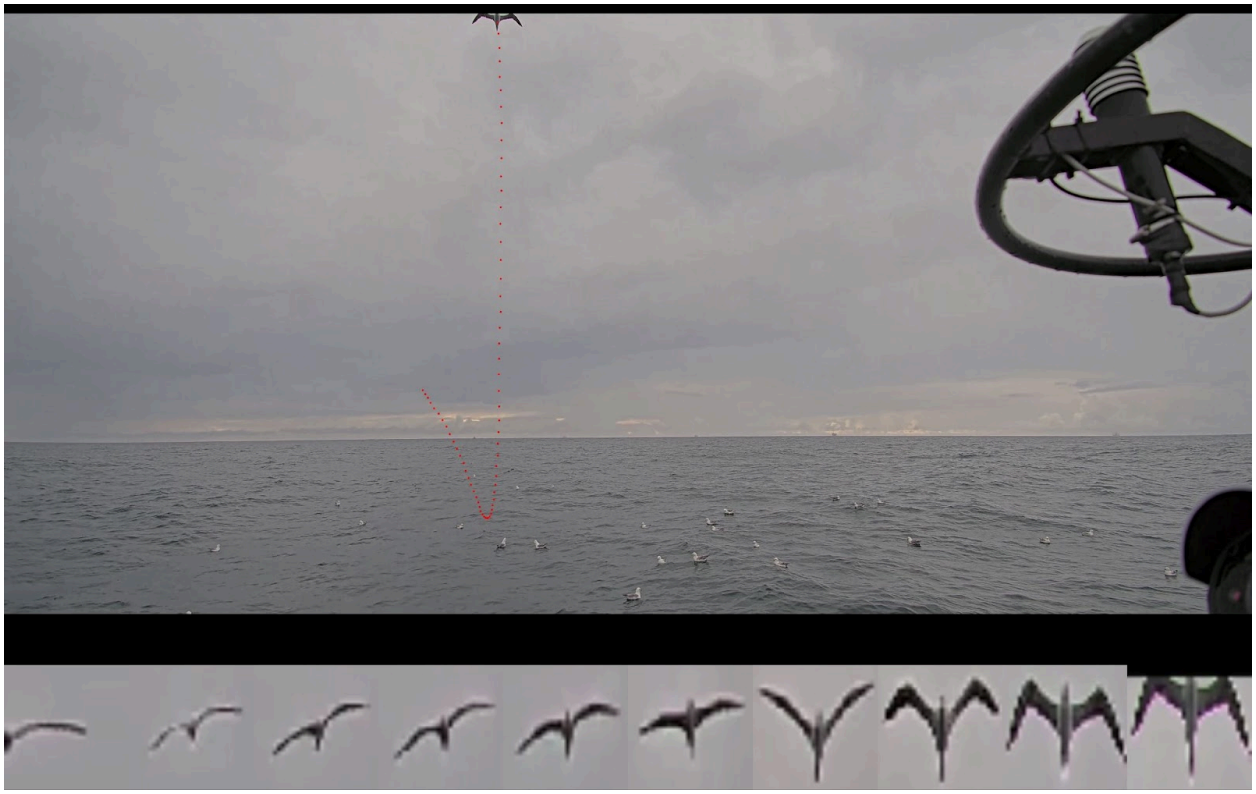

Figure 40: A Northern Gannet captured 29 August 2023. Notice also the at least 25 Northern Fulmars sitting on the ocean surface here as the Northern Gannet passes over. These are tracked individually by the AI.

Other types of movements, like soaring, have been observed by what are most likely local or residential gulls; in particular Great Black-Backed Gulls as the one seen in Figure 41.

Figure 41: A Great Black-backed Gull captured 18 June 2023.

Birds flying in a straight direction during the autumn migration period are likely birds on migration. In addition, the Northern Fulmar and some other seabirds do not migrate linearly, but rather spend the time outside the breeding season cruising the seas and can turn up across most of the North Atlantic.

Figures 34, 36, 37 and 39-41 show examples of birds and their flight tracks, as they are presented in the Spoor webapp. Birds typically appear very small when a video frame is presented as an image, and 10 zoomed-in snapshots of the bird from various points along its flight track are attached at the bottom of each track image. The flight track is indicated in red or green dots superimposed on the image. The flight track is visualised as the bird has appeared in each video frame and thus follows the relative buoy movements. This effect makes the track appear as if the bird has moved more than it actually has.

Note that these images are made for illustrative purposes, and are not the basis for taxonomy classification. In the webapp, the full video segment is available for the viewer to play at their convenience.

Comparing to CCTV results from Hywind Tampen

Spoor conducted a bird monitoring pilot using pre-installed CCTV cameras on three floating turbines on Hywind Tampen from May 2023 to February 2024, which overlapped the full measurement period of this pilot. The results are published in the report *Spoor - AI Avian Monitoring with CCTV Cameras on Floating Wind Turbines (n.d).* Some key metrics are compiled in this chapter in order to compare both the data quality, and the results of the CCTV and buoy-based pilots. The CCTV cameras were mounted 19 metres above the sea line.

Data quality - average detection duration

The average duration of each bird detection was 9.1 seconds for the CCTV vantage points, and 3.4 seconds for the buoy. In other words, each CCTV bird detections lasted on average 2.7 times longer than the buoy bird detections.

Bird activity

For the CCTV pilot, a total of 1,455 bird detections were registered over the full period of 195 days with three cameras, compared to the buoy which saw 55,868 detections over 127 days with four cameras.

The overall detection rates were 0.4 bird detections/recorded hour for CCTV, and 11.4 detections/recorded hour for the buoy - a difference of 2,850%

Peak days of activity

Figure 42 shows the timelines of daily detection rates from the CCTV and buoy, for the measurement period of the buoy pilot. Note that the buoy values were orders of magnitudes higher than the CCTV, and for readability the y-axis of the two timelines have been scaled to allow for visual comparison. The days with the highest detection rates of the CCTV pilot were 25 August 2023 with 3.3 detections per hour, followed by 11 July 2023 with a detection rate of 3.26,and 15 August with a detection rate of 2.23.

21 September, the absolute peak from the buoy vantage point, had an observation rate of only 0.15 from the CCTV vantage points. Note that the number of recorded hours per day for CCTV varied greatly, with some days having no recording time at all. However, the peak days from the CCTV pilot have almost no overlap with the peaks of the buoy pilot.

Figure 42: The timelines of the daily detection rates for CCTV (red) and buoy (purple), respectively. Note that the y-axis of the two timelines are scaled to enable visual comparison of peak days. The detection rates for the buoy are really orders of magnitude larger than those of the CCTV.

Species

50% of all the CCTV pilot detections could be classified to species level, compared to 74% of the subsample in the buoy pilot.

Of the birds that could be classified, 85% were classified as gulls for the CCTV pilot, while 80% were identified as Northern Fulmar for the buoy pilot. Of the buoy pilot detections, only 15% were classified as gulls. The Northern Fulmar only accounted for 1% of the classified birds within the CCTV pilot.

The two species of status endangered and vulnerable were the same for both the CCTV and buoy pilots; the Black-legged Kittiwake and the European Herring Gull.

Flight height

The vantage point of the CCTV cameras were 19 metres above the sea line, and the buoy-based cameras were mounted 3 metres above the sea line. The flight height calculations from the three CCTV cameras showed the main flux from 20 metres to ~70 metres, while the calculations from the buoy-mounted cameras showed a peak at 0-5 metres upwards to 20 metres. In other words, the results of the flight height calculations are almost inverse when comparing the CCTV and buoy pilot results.

Discussion

Data capture has been successful

The cameras functioned uninterrupted during the full measurement period, except for a period of 9 days from 16 - 24 September where Camera 1 was not recording and a period of 2 days from 5 - 6 October when Camera 3 was not recording. No significant issues related to lens contamination by water or salt, sun flare or micro-vibrations were observed. This is especially impressive in the light of the maximum wave heights of 11 m, which demonstrates the durability of the equipment and the persistent ability to detect birds. Although the sun has been in the field of view multiple times, the sun flare effects have not been significant as there has not been substantial contamination on the lens. The reason why contamination has not been an issue, is most likely due to the high quality of the glass and protective film used for the AXIS camera housing. The absence of micro-vibrations shows that the camera mountings have been very robust and that there have been no mechanical vibrations or other types of vibrations that have propagated to the camera equipment.

Downtime in peak period can explain differences in results between camera types

Given the slightly lower monitored volume of the bullet cameras, as per Table 2, it could be expected that the bullet cameras would capture a lower amount of birds compared to the dome cameras. At a first glance of the results in Table 3, that seems to not be the case: The total count of bird detections was higher for the bullet cameras, even as the recorded hours were less compared to the dome cameras.

Two aspects affecting Camera 1 (dome) may have influenced this unexpected result:

- As indicated in Figure 14, Camera 1 had an increase in the number of video files in the period between 7-21 August. The increase probably corresponds to shorter video file lengths, but as the recorded hours are based on the assumption that each file lasts 5 minutes, the number of recorded hours is likely to be exaggerated in this period. The total number of recorded hours for Camera 1 for the measurement period is therefore likely around 110 hours less than indicated in Figure 14 and Table 3, reducing the total recorded time to around 2,370 hours for the two dome cameras. This result is marginally lower than the ~2,400 hours of total recorded time for the bullet cameras.
- Camera 1 was shut off for 9 days during peak activity; 16-24 September. For the other cameras, this period constituted approximately 1/4 of all bird detections in the measurement period. If Camera 1 were active, it can be assumed that birds would be detected in the same magnitude as was seen for Camera 2; which corresponds to ~3,700 detections. The total detection count for the dome cameras would in that case increase to almost 30,000, which is equal to the total detection count of the bullet cameras.

As per Table 3, the total duration of unique bird detections were 25.9 hours and 26.2 hours for the bullet and dome cameras, respectively. If we were to extrapolate the results from Camera 2 to the missing days of Camera 1, it would add around 3,700 bird detections with an average duration of 3.6 seconds, yielding 3.7 hours. The total duration of unique bird detections for dome cameras would increase to 29.9 hours – 15% more than for the bullet cameras. This result correlates with the original hypothesis that the dome cameras would observe more birds due to the larger monitored volume.

Buoy orientation can explain difference in bullet camera results

Table 3 shows that bullet Camera 4 has a 134% higher detection rate compared to bullet Camera 3. The difference in detection rates between the dome camera pair has mainly been explained by the shutoff of Camera 1 during a 9 day peak period, but that explanation does not apply to the bullet camera pair. As seen in Figure 16, the difference is consistently distributed across the measurement period and therefore appears to be systematic. It was also confirmed to be statistically significant by statistical testing.

It was shown that the buoy yaw orientation was northerly and easterly orientation 66% of the time, which means that Camera 4 had a dominating orientation towards south-east and south-west. The corresponding orientations for Camera 3 were south-west and north-west, respectively. Compared to the buoy location as seen in Figure 9, Camera 3 would to a large degree face the directions away from the wind farm, while Camera 4 would have increased exposure towards the wind farm. It can be hypothesised that the difference in detection rates are due to an actual difference in bird activity relative to the wind farm. If so, it would mean that the bird activity was higher within the wind farm relative to the outside of the wind farm. That contradicts findings in the report *Pilot Report. Spoor - AI Avian Monitoring with CCTV Cameras on Floating Wind Turbines. Experiences and Future Potential (2024),* which indicated more bird activity outside of the wind farm compared to within the wind farm. However, the difference in mounting heights of the cameras may play a role. This will be discussed more in the chapter Comparing to CCTV results from Hywind Tampen.

Data quality is affected by buoy movements

For any eulerian sampling type, it is a fact that one cannot know whether the same bird or multiple individual birds are entering and exiting the frame of view. However, this effect is magnified when the observer is moving as well, as is the case with this pilot.

The duration of each bird detection is negatively correlated with wind speed, and the correlation is more pronounced for the buoy compared to the fixed CCTV data as seen in Figures 18 and 19. One explanation for the negative correlation can be an actual difference in bird behaviour at high winds - for example that more birds are active during high winds, or that they fly in a way that makes them enter and exit the field of view more rapidly than at lower winds. However, as the same correlation is not seen in the CCTV data, that would indicate that birds close to sea surface behave differently than birds observed from the CCTV vantage points 19 metres above

the sea. Another explanation could be that high winds make the buoy move in a way that reduces the time that each bird is within the field of view.

Further research could give more answers - but it can be considered likely that a significant part of the correlation is explained by increased buoy movements. If that is the case, then the absolute count of detections are affected by wind speed not representing bird occurrence or behaviour. This makes the metric of bird detections less relevant for the buoy data compared to fixed installations.

Different metrics of bird activity give similar results

The metrics used to measure bird activity in this report are detection count, detection rate, bird minutes and bird minute rate. As the detection rate and bird minute rate accounts for the observed (recorded) time, they are a better expression of relative activity between different time periods.

The number of recorded hours per day were quite constant in this pilot, and as expected, the detection count and detection rates exhibit similar timeline characteristics; lower activity during June and July, slightly increasing in August and peaking in September. The peak at 21 September becomes even more pronounced with the detection rate, seen in Figure 21, compared to the detection count seen in Figure 20, because Camera 1 did not record this day.

Bird minutes is a measure of the total duration that unique birds were detected, not the number of bird detections as such. The number of bird detections can be affected by the buoy movements in different types of weather, and since we are more interested in bird activity and not as interested in effects caused by the buoy movements, the bird minute metric can be a more relevant expression.

In Figure 43, the timelines for the bird minute rate and detection rate are compiled for comparison. Overall the two metrics express similar trends. Both detection rate and bird minute rate display a peak at 21 September. For the purpose of this report, it seems that both metrics are good expressions of observed bird activity.

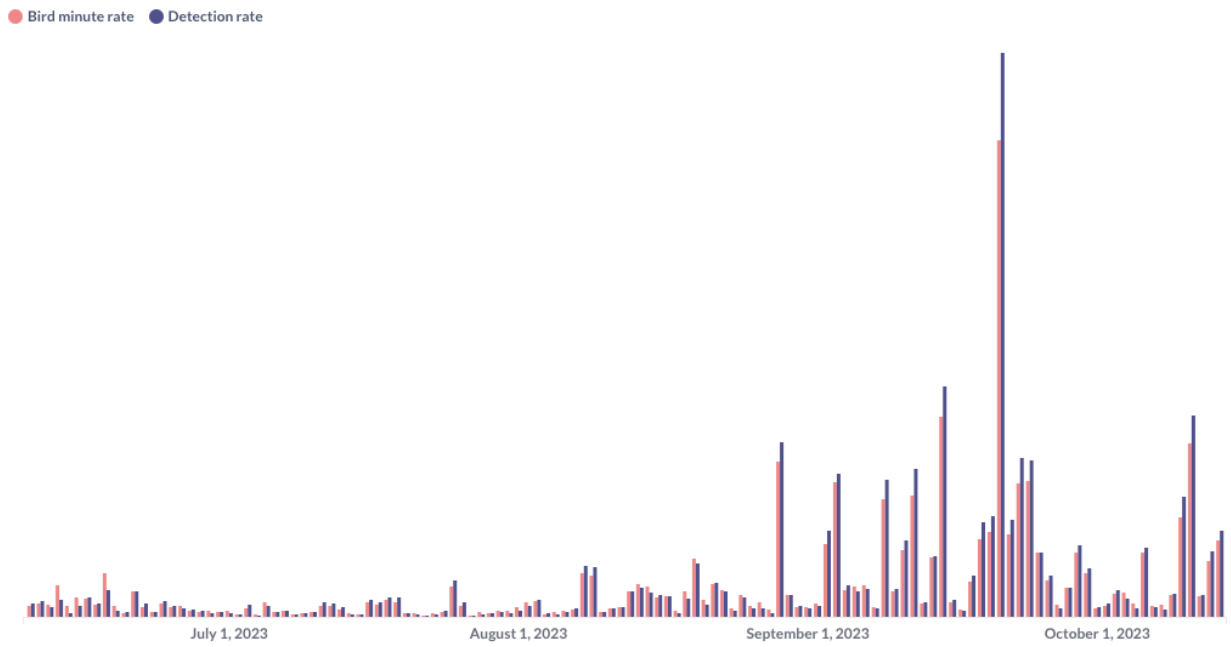

Figure 43: The bird minute rates and detection rates display similar characteristics, indicating that they are comparatively similar metrics.

Bird activity increase during autumn

The highest number of birds are in general expected to be observed after the breeding season; during late summer and autumn, when the new cohort of birds are added to the flying population. Adding to the population during autumn are the migratory birds. This period of increased bird activity is clearly visible in the results of this pilot. The weekly detection rates in Figure 22 rise above the median in the week of 7-13 August. In the daily detection rates in Figure 21, 29 August shows a peak five times above the average for the period. Both these can be a good indicator for the start of the migration period. The pattern of heavily fluctuating activity from day to day is visible throughout September and October in Figure 21 and is a characteristic of migratory activity. This is due to changes in weather conditions, affecting whether or not it is a good day for migration. It should be noted that much of migration activity happens during night, and would thus not have been captured in this pilot.

The highest activity as per Figure 22 is seen in the week of 18-24 September, corresponding to the peak day of 21 September, followed by a decline in detections especially evident in the week of 2-8 October.

The relatively lower activity levels during breeding season and the increase of activity during migration periods are also corroborated by the monthly results in Table 5, showing the highest activity levels in September followed by October, and the lowest activity in July.

The activity throughout the hour of day, as seen in Figure 23, shows a median of around 5 detections per hour. Not surprising, there are a number of high outlier values, reinforcing the results from Figure 21 that bird activity from day to day is so varied that it will not be fully understood by simply averaging over time.

Higher activity at southerly and westerly winds

As per Figure 27 and Table 4, the highest detection rate is observed for southerly winds, followed by westerly winds. The average wind speed for southerly winds and westerly winds were somewhat higher than for the other wind directions. As the majority of observed birds were Northern Fulmar, and these birds use strong winds to fly, this might explain the increase. It is interesting to note that the same trends are seen anecdotally at Utsira, an island at the west coast of Norway. It can be hypothesised that birds prefer to fly when winds are not pushing them too far from the shore or in an undesired direction.

It must also be noted that weather data is retrieved from the Gullfaks C weather station 10 km away from the location, and should be considered only as an approximation.

Peak active days gives insight on conditions for migration

The absolute peak day was 21 September, with a detection rate of 206 detections/hour, 245% more than the second most active day of 84 detections/hour on 15 september. 15 September is only 14% higher than the third most active day of 11 October.

A manual review of all the bird detections for 21 September verified that the majority of observed birds are Northern Fulmars. Northern Fulmars are known to show up in big numbers during migration when the winds and weather conditions are right for them and this is likely one of those days with perfect conditions.

Each of the three peak days are preceded by a five-day period of comparatively low activity, as evident in Figures 31-34. The environmental conditions might explain this pattern. Tables 7-9 shows that two of the peak days have no precipitation, while the prior day had precipitation. 11 October has precipitation, but the day before had more precipitation. This can indicate that a reduction in precipitation might be beneficial for migration.

The wind speeds are comparatively high in all the three peak days, and the prior days have lower winds speeds. It may indicate that migration peaks happen with increase of wind speed. Furthermore, there seems to be a shift in wind direction but this does not appear to be systematic. The three peak days saw daily average wind directions from south, from south-west, and from west, respectively - corroborating the results in Table 4 showing the highest activity during westerly and southerly winds. It is also worth noting that 11 October was the day with the highest average wind speed in the whole measurement period.

Northern Fulmar is the most observed species

Five species were identified in the sample, all of them seabirds. The endangered Black-legged Kittiwake was only detected in one instance, but at long ranges it is harder to differentiate the exact species of gulls, and it can be assumed that more of this species is within the category of unidentified gulls. The same is true for the European Herring Gull. Curiously, one detection of a small passerine bird was made in July, outside of the migration period and far offshore for a land-based bird. This is most likely a stray bird. Loons are also not seabirds per se, but spend large parts of their year offshore and is less surprising to observe.

Northern Fulmars was by far the most occurring species. According to *Norsk Polarinstitutt: Northern Fulmar* (n.d.); this species glides over the sea just above the surface on stiff, straight wings, and floats high in the water when swimming. The cameras on the buoy, 3 metres above the sealine, therefore have excellent conditions to detect the Northern Fulmars both on the sea and in air.

Table 13 shows that the Northern Fulmar accounts for less than 50% of the classified birds during the summer months, and increases substantially during the autumn months. The same trend is seen for the absolute counts in Table 12. This is as expected, as most Northern Fulmars would be closer to the breeding grounds further north during summer (breeding season) and more dispersed at sea during migration (autumn and winter). Northern Gannets – the largest seabird in the North Atlantic – would be expected to show the same trend of lower abundance during the breeding season, but the opposite is observed. However, the number of detections are too low to know if they accurately represent true abundance. The Northern Gannets that were detected during summer might be non-breeding individuals.

Flight height densities higher close to the sea surface

Due to the constantly moving nature of the fields of view in this pilot, Spoor had to develop a novel method for calculating the flight heights. The results show the highest flight height densities of 0-20 metres above the sea. The bias of distance decay of detections are present; i.e. that birds closer to the observer have a higher probability of detection, and this has not been corrected for in Figures 28-30. Further, the patterns of the dome cameras in Figure 29 and the bullet cameras in Figure 30 show small differences between the camera types. The bullet cameras show the highest densities in the altitudes of 0-10 metres, while the dome cameras show a broader distribution of densities between 0-20 metres. This is most likely due to effects of the cameras that can be corrected for.

Mounting heights can explain differences in CCTV and buoy results

The results from the buoy-mounted cameras of this pilot, and the results from the CCTV pilot are collected from the same time period and from the same area, but exhibit substantial differences in a number of ways:

1. The sheer number of detections, and the detection rates, are orders of magnitude higher for the buoy-mounted cameras compared to the CCTV results. Buoy-mounted cameras had an average of 12.9 detections per hour, while the CCTV cameras had approximately 0.5 detections per hour.
2. There is a difference in the days of peak activity between the CCTV pilot and the buoy pilot.
3. For the buoy pilot, the Northern Fulmar was the dominating species, while gulls were dominating in the CCTV pilot.
4. The buoy pilot had highest detection rates for southerly and westerly winds, while the CCTV pilot had highest detection rates for northerly winds.
5. The calculated flight height of the buoy-based cameras have highest density 0-20 metre altitudes, while the CCTV pilot showed highest densities at 20-60 metre altitudes.
6. The buoy pilot results hints to higher detection rates within the wind farm - while CCTV indicated highest detection rate outside the wind farm.

In addition, problems with sun flare, water droplets and contamination was a problem in the CCTV pilot, and has not been problematic in the buoy-based pilot.

One of the key differences between the CCTV pilot and the buoy pilot were the mounting height of the cameras; 19 metres compared to 3 metres above the sea. The former are better positioned to capture birds in-flight and have not been able to capture birds close to or resting on the sea. We can expect different behaviour close to sea surface compared to in the airspace, and also different species. The Northern Fulmar is known to fly near the sea surface and would not be expected to be frequently seen at altitudes of 19 metres and more.

Other factors that may leads to the differences in results:

- The algorithm used in the buoy-based pilot could capture resting birds on the sea, as opposed to the algorithm used for the CCTV pilot. In effect, due to the position of the cameras and the detection ability of the algorithms, the two pilots have been monitoring almost mutually exclusive altitudes.
- The average detection duration for the buoy-based cameras were ⅓ compared to the fixed CCTV cameras. It indicates that the movements of the buoy-based cameras contribute to shorter and more numerous bird detections, compared to the CCTV.
- The buoy might have had an attractive effect on birds wanting to use it as a rest. If so, the bird directions have been “artificially” increased.

Reflections and learnings

The difference between a fixed and moving vantage point

The nature of the moving buoy means that the monitored volume and orientation is constantly changing. This is a significant difference to other camera-based monitoring campaigns, where cameras remain fixed on a stable mount and the monitored volume is constant. Spoor has developed novel methods to detect and track birds, and methods for interpreting the results. However, further work is needed to explore both the uncertainties and possibilities of the data.

The need for offshore industry standards on performance levels

The introduction of novel technologies to gather biodiversity data offshore raises the question of how best to develop standardised methodologies and performance measurements. Traditional ground-truthing using human observers is the de facto standard approach, but this method itself contains numerous biases and limitations so it has questionable utility when evaluating new techniques. In the case of buoys in particular, it is hugely impractical to gather useful human ground-truth data in the same areas for any significant length of time, and particularly under varied and rough weather conditions.

Practical implementation

The collaboration between Equinor, Fugro and Spoor has been very good, and a key element of this success has been the direct and unobstructed communication, especially between technical staff on both sides. Further, Fugro made qualified technical staff available, with the right mandate to solve issues as they arose. The support and availability of environmental and biological experts in Equinor have also been immensely beneficial for execution and implementation.

Fugro designed the hardware setup and installed the cameras and the data storage hardware. It needs to be retro-fitted to not obstruct the other sensors that capture wind-, wave-, current- and other data. Some recommendations for the next implementation is to synchronise cameras from the start, to assess the actual need for RAID (redundant array of independent disks) setup – as storage capacity may be doubled if it is not needed – and in general investigate low-power components to allow for longer deployments.

Next steps

Improving AI performance

For this project Spoor has adopted their AI computer vision software to handle deployments where cameras are mounted on a moving platform and also added the ability to detect birds that appear in front of the sea. Further iterations sampling training data, training and tuning the model, and hyper-parameter searches would yield a model with even better performance, with improved ability to detect birds in front of sea, and increase the range of detections and therefore also the area monitored and in general to improve the performance of this model.

Qualitative analysis of bird behaviour

If it is of biological interest, it would be possible to distinguish between resting birds and birds in-flight. Furthermore, the visual bird tracks represented in the webapp can be stabilised to reduce the apparent effect of the buoy movement.

Further insight can also be retrieved about the conditions for migration, especially if local weather is collected.

Measuring flight direction

In order to accurately know the flight direction of each bird, Spoor needs granular compass data from the buoy. As a default, Fugro samples the buoy orientation each second, and stores the data as mean, maximum and minimum yaw (orientation) values at 10 minute intervals. This is ideal for calculating wave direction statistics, but not for the purpose of measuring flight directions of birds.

For future deployments, it is possible to calculate a regular 1Hz time series from the data, with an expected uncertainty of the timestamp in the range of a few seconds. It will also require time-synchronisation between all the cameras.

Statistical analysis of results

There are two key challenges that must be overcome when estimating the spatial distribution of birds from camera data. Firstly, it is necessary to correct for the volume of space surveyed, and secondly, it is necessary to account for decreasing detection probability with distance. The surveyed volume is a new challenge in this deployment, as the monitored volume constantly varies. In regards to the decreasing detection probability with distance, Spoor and Vattenfall have engaged the British Trust for Ornithology (BTO) to develop a model for flux based on fixed Spoor AI data. The results are expected to be published in the second half of 2024.

Reducing data storage

Almost 60% of the available data storage was used for this 127 day measurement period. For campaigns with longer duration, it is important to increase the amount of available data storage, and/or reduce the need for data storage.

The number of recorded hours per day was set to around 10 hours per camera for this pilot. It is possible to program the cameras to record for a shorter daily time period, which would reduce the daily data generation and reduce the data storage requirements.

Edge processing - on-site bird detection and tracking - would lower the requirement to store raw data, as the AI analysis would be done locally and only the results and not the raw data would need to be stored.

Reducing power consumption

All in all the Spoor equipment required 72 W, which needs to be reduced when moving from a pilot deployment to a full-length deployment with limited maintenance access. AXIS has released new, power-efficient dome cameras that are going to greatly reduce the total power consumption. Reducing the number of cameras is another option for long-term deployments.

Conclusion

This pilot has demonstrated the potential for using camera sensors on floating lidar buoys and other floating platforms, to capture large volumes of bird activity data offshore in areas which would otherwise be extremely difficult and prohibitively expensive to monitor using traditional methods. The pilot has also delivered insight and learnings that can be incorporated into a roadmap for further development.

This novel method of collecting high-resolution, site-specific, bird data will help build a solid foundation of empirical evidence to enable more accurate environmental impact assessments in the planning and permitting phases of windfarm development. These data will also provide a baseline which can be correlated against bird-monitoring data captured over the operational lifetime of a wind farm. All of this combined will help to reduce the environmental and financial risk of offshore wind development, as well as contributing to the scientific knowledge base in this rapidly evolving field.

Acknowledgements

Spoor wants to particularly thank Kari Mette Murvoll from Equinor for leading the excellent collaboration at every stage of this project, as well as her colleagues Tonje Waterloo Rogstad and Arne Myhrvold for their expert support. In addition, we are very grateful to Inés Martín Grandes, Felix Kelberlau and Vegar Neshaug from Fugro, and all of the above named from both organisations for their commitment to collaborative innovation.

References

- *Artsdatabanken: Norsk rødliste for arter 2021* (2021). Available at: https://artsdatabanken.no/lister/rodlisteforarter/2021 (Accessed: 28 March 2024)
- *AXIS Q1798-LE Network Camera (n.d)*. Available at: https://www.axis.com/products/axis-q1798-le (Accessed 7 May 2024)
- *AXIS Q3538-SLVE Dome Camera (n.d).* Available at: https://www.axis.com/products/axis-q3538-slve (Accessed 7 May 2024)
- *Evidently AI: Accuracy vs. precision vs. recall in machine learning: what's the difference?* (n.d). Available at: https://www.evidentlyai.com/classification-metrics/accuracy-precision-recall (Accessed: 28 March 2024)
- *Equinor: Hywind Tampen* (n.d). Available at: https://www.equinor.com/energy/hywind-tampen (Accessed: 28 March 2024)
- *Global Biodiversity Information Facility: What is Darwin Core, and Why does it matter?* (n.d.). Available at: https://www.gbif.org/darwin-core (Accessed: 5 April 2024)
- *Norsk Polarinstitutt: Northern Fulmar* (n.d.). Available at: https://www.npolar.no/en/species/northern-fulmar/ (Accessed: 29 May 2024)
- Phillips et al. (2019). "Does perspective matter? A case study comparing Eulerian and Lagrangian estimates of common murre (Uria aalge) distributions. Ecology and Evolution, 9 (8), p.p. 4805-4819. https://doi.org/10.5061/dryad.1hg2n56.
- *Pilot Report. Spoor - AI Avian Monitoring with CCTV Cameras on Floating Wind Turbines. Experiences and Future Potential* (2024). [Report pending publication]
- *The Royal Society for the Protection of Birds: Great Black-backed Gull* (n.d.). Available at: https://www.rspb.org.uk/birds-and-wildlife/great-black-backed-gull (Accessed 28 March 2024)
- *The Norwegian Centre for Climate Services: Observations and weather statistics* (n.d.). Available at: https://seklima.met.no/minutes/wind_from_direction/custom_period/SN76923/en/2023-05-01T00:00:00+02:00;2024-03-28T14:21:59+01:00 (accessed 28 March 2024)
- Zhang *et al.* (2014). An Implementation of Document Image Reconstruction System on a Smart Device Using a 1D Histogram Calibration Algorithm. Mathematical Problems in Engineering. 2014. 1-10. 10.1155/2014/313452.